

CHAPTER 1

COLOR SUPERCONDUCTIVITY IN DENSE, BUT NOT
ASYMPTOTICALLY DENSE, DENSE QUARK MATTER

Mark Alford

Physics Department, Washington University
Saint Louis, MO 63130, USA

Krishna Rajagopal

Center for Theoretical Physics, Massachusetts Institute of Technology
Cambridge, MA 02139 USA
Nuclear Science Division, Lawrence Berkeley National Laboratory
Berkeley, CA 94720, USA

At ultra-high density, matter is expected to form a degenerate Fermi gas of quarks in which there is a condensate of Cooper pairs of quarks near the Fermi surface: color superconductivity. In this chapter we review some of the underlying physics, and discuss outstanding questions about the phase structure of ultra-dense quark matter. We then focus on describing recent results on the crystalline color superconducting phase that may be the preferred form of cold, dense but not asymptotically dense, three-flavor quark matter. The gap parameter and free energy for this phase have recently been evaluated within a Ginzburg-Landau approximation for many candidate crystal structures. We describe the two that are most favorable. The robustness of these phases results in their being favored over wide ranges of density. However, it also implies that the Ginzburg-Landau approximation is not quantitatively reliable. We describe qualitative insights into what makes a crystal structure favorable which can be used to winnow the possibilities. We close with a look ahead at the calculations that remain to be done in order to make quantitative contact with observations of compact stars.

1. Introduction

The exploration of the phase diagram of matter at ultra-high temperature or density is an area of great interest and activity, both on the experimental and theoretical fronts. Heavy-ion colliders such as the SPS at CERN and RHIC at Brookhaven have probed the high-temperature region, creating and studying the properties of quark matter with very high energy density and very low baryon number density similar to the quid which filled the universe for the first microseconds after the big bang. In this paper we discuss a different part of the phase diagram, the low-temperature high-density region. Here there are as yet no experimental constraints, and our goal is to

understand the properties of matter predicted by QCD well enough to be able to use astronomical observations of neutron stars to learn whether these densest objects in the current universe contain quark matter in their core. We expect cold, dense, matter to exist in phases characterized by Cooper pairing of quarks, i.e. color superconductivity, driven by the Bardeen-Cooper-Schrieffer (BCS)¹ mechanism. The BCS mechanism operates when there is an attractive interaction between fermions at a Fermi surface. The QCD quark-quark interaction is strong, and is attractive in many channels, so we expect cold dense quark matter to generically exhibit color superconductivity. Moreover, quarks, unlike electrons, have color and flavor as well as spin degrees of freedom, so many different patterns of pairing are possible. This leads us to expect a rich phase structure in matter beyond nuclear density.

Calculations using a variety of methods agree that at sufficiently high density, the favored phase is color-flavor-locked (CFL) color-superconducting quark matter² (for reviews, see Ref. 3). However, there is still uncertainty over the nature of the next phase down in density. Previous work^{4;5} had suggested that when the density drops low enough so that the mass of the strange quark can no longer be neglected, there is a continuous phase transition from the CFL phase to a new gapless CFL (gCFL) phase, which could lead to observable consequences if it occurred in the cores of neutron stars.⁶ However, it now appears that some of the gluons in the gCFL phase have imaginary Meissner masses, indicating an instability towards a lower-energy phase.^{7;8;9;10;11;12;13;14;15;16;17;18} A analysis in the vicinity of the unstable gCFL phase cannot determine the nature of the lower-energy phase that resolves the instability. However, the instability is telling us that the system can lower its energy by turning on currents, suggesting that the crystalline color superconducting phase,¹⁹ in which the condensate is modulated in space in a way that can be thought of as a sum of counterpropagating currents, is a strong candidate.

2. Review of color superconductivity

2.1. Color superconductivity

The fact that QCD is asymptotically free implies that at sufficiently high density and low temperature, there is a Fermi surface of weakly-interacting quarks. The interaction between these quarks is certainly attractive in some channels (quarks bind together to form baryons), so we expect the formation of a condensate of Cooper pairs. We can see this by considering the grand canonical potential $\Omega = (E - \mu N)/V$, where E is the total energy of the system, μ is the chemical potential, and N is the number of quarks. The Fermi surface is defined by a Fermi energy $E_F = \mu$, at which the free energy is minimized, so adding or subtracting a single particle costs zero free energy. Now switch on a weak attractive interaction. It costs no free energy to add a pair of particles (or holes), and if they have the right quantum numbers then the attractive interaction between them will lower the free energy of the system. Many such pairs will therefore be created in the modes near the Fermi surface, and these pairs, being bosonic, will form a condensate. The ground state

will be a superposition of states with all numbers of pairs, breaking the fermion number symmetry.

A pair of quarks cannot be a color singlet, so the resulting condensate will break the local color symmetry $SU(3)_{\text{color}}$. The formation of a condensate of Cooper pairs of quarks is therefore called "color superconductivity". The condensate plays the same role here as the Higgs condensate does in the standard model: the color-superconducting phase can be thought of as the Higgs phase of QCD.

2.2. Highest density: Color-flavor locking (CFL)

It is by now well-established that at sufficiently high densities, where the up, down and strange quarks can be treated on an equal footing and the disruptive effects of the strange quark mass can be neglected, quark matter is in the color-flavor locked (CFL) phase, in which quarks of all three colors and all three flavors form conventional Cooper pairs with zero total momentum, and all fermionic excitations are gapped, with the gap parameter $\mu_0 \sim 10-100 \text{ MeV}$.^{2,3} This has been confirmed by both NJL^{2;20;3} and gluon-mediated interaction calculations.^{21;22;23;3} The CFL pairing pattern is²

$$\chi_{ij} C_{5q_j i} = \delta_{ij} + \delta_{ij} = \delta_{ij} \quad (1)$$

$$[SU(3)_{\text{color}}] \times [SU(3)_L \times SU(3)_R \times U(1)_B] \rightarrow [SU(3)_{\text{CFL}} \times U(1)_C] \quad (1)$$

Color indices i, j and flavor indices i, j run from 1 to 3, Dirac indices are suppressed, and C is the Dirac charge-conjugation matrix. The term multiplied by corresponds to pairing in the $(6_S; 6_S)$, which although not energetically favored breaks no additional symmetries and so is in general small but nonzero.^{2;21;22;24} The Kronecker δ 's connect color indices with flavor indices, so that the condensate is not invariant under color rotations, nor under flavor rotations, but only under simultaneous, equal and opposite, color and flavor rotations. Since color is only a vector symmetry, this condensate is only invariant under vector flavor+color rotations, and breaks chiral symmetry. The features of the CFL pattern of condensation are²

The color gauge group is completely broken. All eight gluons become massive. This ensures that there are no infrared divergences associated with gluon propagators.

All the quark modes are gapped. The nine quarks (three colors times three flavors) fall into an $8+1$ of the unbroken global $SU(3)$. Neglecting corrections of order μ_0 (see (1)) the octet and singlet quarks have gap parameter μ_0 and $2\mu_0$ respectively.

A rotated electromagnetic gauge symmetry (generated by Q) survives unbroken. The single remaining massless gauge boson is a linear combination of the original photon and one of the gluons.

Two global symmetries are broken, the chiral symmetry and baryon number, so there are two gauge-invariant order parameters that distinguish the CFL phase from the QGP, and corresponding Goldstone bosons which are long-wavelength disturbances of the order parameter. When the light quark mass is nonzero it explicitly breaks the chiral symmetry and gives a mass to the chiral Goldstone octet, but the CFL phase is still a superfluid, distinguished by its spontaneous baryon number breaking.

2.3. Less dense quark matter: stresses on the CFL phase

The CFL phase is characterized by pairing between different flavors and different colors of quarks. We can easily understand why this is to be expected. Firstly, the QCD interaction between two quarks is most attractive in the channel that is antisymmetric in color (the $\bar{3}$). Secondly, pairing tends to be stronger in channels that do not break rotational symmetry,^{25;26;27;28;29;30} so we expect the pairs to be spin singlets, i.e. antisymmetric in spin. Finally, fermionic antisymmetry of the Cooper pair wavefunction then forces the Cooper pair to be antisymmetric in flavor.

Pairing between different colors/ flavors can occur easily when they all have the same chemical potentials and Fermi momenta. This is the situation at very high density, where the strange quark mass is negligible. However, even at the very center of a compact star the quark number chemical potential cannot be much larger than 500 MeV, meaning that the strange quark mass M_s (which is density dependent, lying somewhere between its vacuum current mass of about 100 MeV and constituent mass of about 500 MeV) cannot be neglected. Furthermore, bulk matter, as relevant for a compact star, must be in weak equilibrium and must be electrically and color neutral^{31;32;33;34;35;36} (possibly via mixing of oppositely charged phases). All these factors work to separate the Fermi momenta of the three different flavors of quarks, and thus disfavor the cross-species BCS pairing that characterizes the CFL phase. If we imagine beginning at asymptotically high densities and reducing the density, and suppose that CFL pairing is disrupted by the heaviness of the strange quark before color superconducting quark matter is superseded by baryonic matter, the CFL phase must be replaced by some phase of quark matter in which there is less, and less symmetric, pairing.

In the next few subsections we give a quick overview of the expected phases of real-world quark matter. We restrict our discussion to zero temperature because the critical temperatures for most of the phases that we discuss are expected to be of order 10 MeV or higher, and the core temperature of a neutron star is believed to drop below this value within minutes (if not seconds) of its creation in a supernova.

2.4. Kaon condensation: the CFL-K⁰ phase

Bedaque and Schafer^{37;38} showed that when the stress is not too large (high density), it may simply modify the CFL pairing pattern by inducing a flavor rotation

of the condensate which can be interpreted as a condensate of K^0 mesons, i.e. the neutral anti-strange Goldstone bosons associated with the chiral symmetry breaking. This is the $\backslash\text{CFL-}K^0$ phase, which breaks isospin. The K^0 -condensate can easily be suppressed by instanton effects,³⁹ but if these are ignored then the kaon condensation occurs for M_s & $m^{1=3} = m^{2=3}$ for light (u and d) quarks of mass m . This was demonstrated using an effective theory of the Goldstone bosons, but with some effort can also be seen in an NJL calculation.^{40;41}

2.5. The gapless CFL phase

The nature of the next significant transition has been studied in NJL model calculations which ignore the K^0 -condensation in the CFL phase and which assume spatial homogeneity.^{4;5;42;43;44;45;46;47} It has been found that the phase structure depends on the strength of the pairing. If the pairing is sufficiently strong (so that $\mu_0 \approx 100$ MeV where μ_0 is what the CFL gap would be at $\mu = 500$ MeV if M_s were zero) then the CFL phase survives all the way down to the transition to nuclear matter. For a wide range of parameter values, however, we find something more interesting. We can make a rough quantitative analysis by expanding in powers of $M_s^2 = \mu^2$ and $\mu = \mu_0$, and ignoring the fact that the effective strange quark mass may be different in different phases.³³ Such an analysis shows that, within a spatially homogeneous ansatz, as we come down in density we find a transition at $\frac{1}{2}M_s^2 = \mu_0^2$ from CFL to another phase, the gapless CFL phase (gCFL).^{4;5} In this phase, quarks of all three colors and all three flavors still form ordinary Cooper pairs, with each pair having zero total momentum, but there are regions of momentum space in which certain quarks do not succeed in pairing, and these regions are bounded by momenta at which certain fermionic quasiparticles are gapless. This variation on BCS pairing | in which the same species of fermions that pair feature gapless quasiparticles | was first proposed for two flavor quark matter^{48;49} and in an atomic physics context.⁵⁰

For $M_s^2 = \mu^2$ & $2\mu_0^2$, the CFL phase has higher free energy than the gCFL phase. This follows from the energetic balance between the cost of keeping the Fermi surfaces together and the benefit of the pairing that can then occur. The leading effect of M_s is like a shift in the chemical potential of the strange quarks, so the bd and gs quarks feel "effective chemical potentials" $\mu_{bd} = \frac{2}{3}\mu_s$ and $\mu_{gs} = \mu_s + \frac{1}{3}\mu_s = \frac{4}{3}\mu_s$. In the CFL phase $\mu_s = M_s^2/(2\mu_0^2)$,^{33;34} so $\mu_{bd} = \mu_{gs} = M_s^2/(2\mu_0^2)$. The CFL phase will be stable as long as the pairing makes it energetically favorable to maintain equality of the bd and gs Fermi momenta, despite their differing chemical potentials.^{51;4} It becomes unstable when the energy gained from turning a gs quark near the common Fermi momentum into a bd quark (namely $M_s^2/(2\mu_0^2)$) exceeds the cost in lost pairing energy $2\mu_0$. So the CFL phase is stable when

$$\frac{M_s^2}{\mu_0^2} < 2\mu_0 : \quad (2)$$

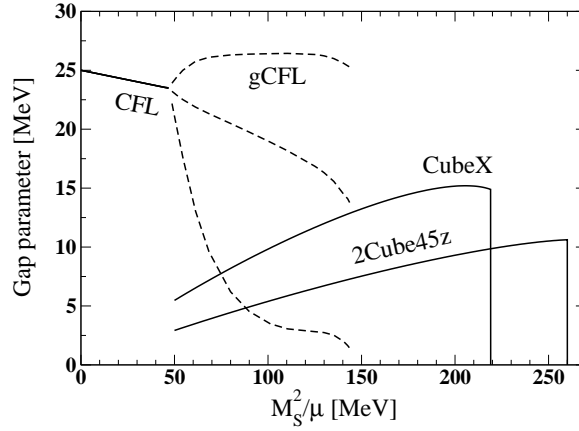


Fig. 1. Gap parameter versus $M_s^2 =$ for the CFL and gCFL phases as well as for crystalline color superconducting phases with two different crystal structures described in Section 3.6. These gap parameters have all been evaluated in a NJL model with the interaction strength chosen such that the CFL gap parameter is 25 MeV at $M_s^2 = 0$. In the gCFL phase, $u_d > u_s > d_s$. The calculation of the gap parameters in the crystalline phases has been done in a Ginzburg-Landau approximation. Recall that the splitting between Fermi surfaces is proportional to M_s^2 , and that small (large) M_s^2 corresponds to high (low) density.

Including the effects of K^0 -condensation expands the range of M_s^2 in which the CFL phase is stable by a few tens of percent.^{38;40;41} For larger M_s^2 , the CFL phase is replaced by some new phase with unpaired b-d quarks, which cannot be neutral unpaired or 2SC quark matter because the new phase and the CFL phase must have the same free energy at the critical $M_s^2 = M_{s0}^2$.

The obvious approach to finding this phase is to perform a NJL model calculation with a general ansatz for the pairing that includes differences between the flavors, for example by allowing different pairing strengths u_d, d_s, u_s . This was done in Refs. 4, 5, and the resultant "gCFL" phase was described in detail. In Figs. 1 and 2 we show the results. The gCFL phase takes over from CFL at $M_s^2 = M_{s0}^2$, and remains favored beyond the value $M_s^2 = M_{s40}^2$ at which the CFL phase would become unfavored.

2.6. Beyond gapless CFL

The arguments above led us to the conclusion that the favored phase of quark matter at the highest densities is the CFL phase, and that as the density is decreased there is a transition to another color superconducting phase, the gapless CFL phase. However, it turns out that the gCFL phase is itself unstable, and that in the regime where the gCFL phase has a lower free energy than both the CFL phase and unpaired quark matter, there must be some other phase with lower free energy still. The nature of that phase has to date not been determined rigorously, and in subsequent subsections we shall discuss various possibilities. However, the

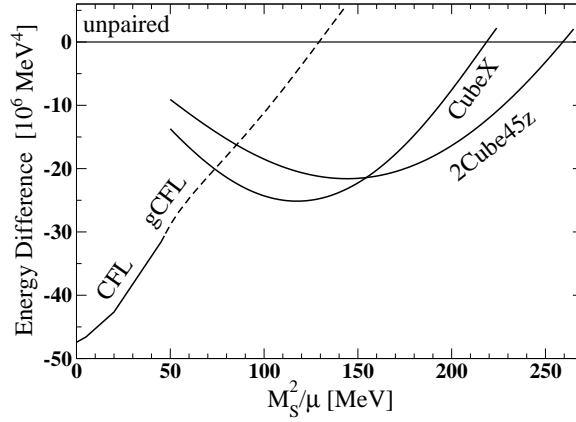


Fig. 2. Free energy relative to that of neutral unpaired quark matter versus $M_s^2 =$ for the CFL, gCFL and crystalline phases whose gap parameters are plotted in Fig. 1. Recall that the gCFL phase is known to be unstable, meaning that in the regime where the gCFL phase free energy is plotted, the true ground state of three-flavor quark matter must be some phase whose free energy lies below the dashed line. We see that the three-flavor crystalline color superconducting quark matter phases with the most favorable crystal structures that we have found, namely 2Cube45z and CubeX described in (31) and (33), have sufficiently robust condensation energy (sufficiently negative) that they are candidates to be the ground state of matter over a wide swath of $M_s^2 =$, meaning over a wide range of densities.

crystalline color superconducting phases analyzed very recently in Ref. 52 whose free energies are shown in Fig. 2 appear particularly robust, offering the possibility that over a wide range of densities they are the ground state of dense matter. We shall therefore discuss these phases at much greater length in Section 3.

In all the contexts in which they have been investigated (whether in atomic physics or the g2SC phase in two-flavor quark matter or the gCFL phase) the gapless paired state turns out to suffer from a “magnetic instability”: it can lower its energy by the formation of counter-propagating currents.^{7;8;9;10;11;12;13;14;15;16;17;18} In the atomic physics context, the resolution of the instability is phase separation into macroscopic regions of two phases in one of which standard BCS pairing occurs and in the other of which no pairing occurs.^{53;54;55} Phase separation into electrically charged but color neutral phases is also a possibility in two-flavor quark matter.⁵⁶ In three-flavor quark matter, where the instability of the gCFL phase has been established in Refs. 8, 12, phase coexistence would require coexisting components with opposite color charges, in addition to opposite electric charges, making it very unlikely that a phase separated solution can have lower energy than the gCFL phase.^{5;42} Furthermore, color superconducting phases which are less symmetric than the CFL phase but still involve only conventional BCS pairing, for example the much-studied 2SC phase in which only two colors of up and down quarks pair^{57;58;59} but including also many other possibilities,⁶⁰ cannot be the resolution of the gCFL instability.^{33;60} It seems likely, therefore, that a ground

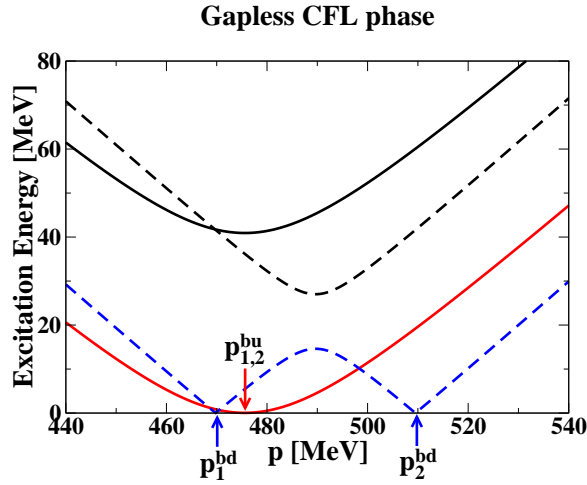


Fig. 3. Dispersion relations of the lightest quasiquark excitations in the gCFL phase, at $\mu = 500$ MeV, with $M_s = 200$ MeV and interaction strength such that the CFL gap parameter at $M_s = 0$ would be $\mu_0 = 25$ MeV. Note that in there is a gapless mode with a quadratic dispersion relation (energy reaching zero at momentum $p_{1,2}^{bu}$) as well as two gapless modes with more conventional linear dispersion relations.

state with counter-propagating currents is required. This could take the form of a crystalline color superconductor^{19;61;62;63;64;65;66;67;68;69;70;71;52} | the QCD analogue of a form of non-BCS pairing first considered by Larkin, Ovchinnikov, Fulde and Ferrell.⁷² Or, given that the CFL phase itself is likely augmented by kaon condensation,^{37;38;40;41} it could take the form of a phase in which a CFL kaon condensate carries a current in one direction balanced by a counter-propagating current in the opposite direction carried by gapless quark quasiparticles.^{14;18}

The instability of the gCFL phase appears to be related to one of its most interesting features, namely the presence of gapless fermionic excitations around the ground state. These are illustrated in Fig. 3, which shows that there is one mode (the burs quasiparticle) with an unusual quadratic dispersion relation, which is expected to give rise to a parametrically enhanced heat capacity and neutrino emissivity and anomalous transport properties.⁶ The instability manifests itself in imaginary Meissner masses M_M for some of the gluons. M_M^2 is the low-momentum current-current two-point function, and $M_M^2 = (g^2 - \kappa^2)$, with g the gauge coupling, is the coefficient of the gradient term in the effective theory of small fluctuations around the ground-state condensate. The fact that we find a negative value when the quasiparticles are gapless indicates an instability towards spontaneous breaking of translational invariance. Calculations in a simple two-species model¹⁰ show that imaginary M_M is generically associated with the presence of gapless charged fermionic modes.

The earliest calculations for the three-flavor case show that even a very simple

ansatz for the crystal structure yields a crystalline color superconducting state that has lower free energy than gCFL in the region where the gCFL \rightarrow unpaired transition occurs.^{69;71} It is reasonable, based on what was found in the two-flavor case in Ref. 65, to expect that when the full space of crystal structures is explored, the crystalline color superconducting state will be preferred to gCFL over a much wider range of the stress parameter $M_s^2 = (\sigma/\mu)$, and this expectation has recently been confirmed by explicit calculation.⁵² It is conceivable that the whole gCFL region is actually a crystalline region, but the results shown in Fig. 2 that we describe in Section 3 suggest that there is still room for other possibilities (like the current-carrying meson condensate) at the highest densities in the gCFL regime.

An alternative explanation of the consequences of the gCFL instability was advanced by Hong⁷³ (see also Ref. 49): since the instability is generically associated with the presence of gapless fermionic modes, and the BCS mechanism implies that any gapless fermionic mode is unstable to Cooper pairing in the most attractive channel, one might expect that the instability will simply be resolved by "secondary pairing". This means the formation of a hqqi condensate where q is either one of the gapless quasiparticles whose dispersion relation is shown in Fig. 3. After the formation of such a secondary condensate, the linear gapless dispersion relations would be modified by "rounding out" of the corner where the energy falls to zero, leaving a secondary energy gap Δ_s , which renders the mode gapped, and removes the instability. In the case of the quadratically gapless mode there is a greatly increased density of states at low energy (in fact, the density of states diverges as $E^{-1/2}$), so Hong calculated that the secondary pairing should be much stronger than would be predicted by BCS theory, and he specifically predicted Δ_s / G_s^2 for coupling strength G_s , as compared with the standard BCS result $\Delta / \exp(-\text{const}/G_s)$.

This possibility was worked out in a two-species NJL model in Ref. 74. This allowed a detailed exploration of the strength of secondary pairing. The calculation confirmed Hong's prediction that in typical secondary channels Δ_s / G_s^2 . However, in all the secondary channels that were analyzed it was found that the secondary gap, even with this enhancement, is from ten to hundreds of times smaller than the primary gap at reasonable values of the secondary coupling. This shows that that secondary pairing does not generically resolve the magnetic instability of the gapless phase, since it indicates that there is a temperature range $\Delta_s \leq T \leq T_p$ in which there is primary pairing (of strength Δ_p) but no secondary pairing, and at those temperatures the instability problem would arise again.

2.7. Crystalline pairing

The pairing patterns discussed so far have been translationally invariant. But in the region of parameter space where cross-species pairing is excluded by stresses that pull apart the Fermi surfaces, one expects a position-dependent pairing known as the crystalline color superconducting phase.^{72;19;61;62;63;64;65;66;67;68;69;70;71;52} This arises because one way to achieve pairing between different flavors while accom-

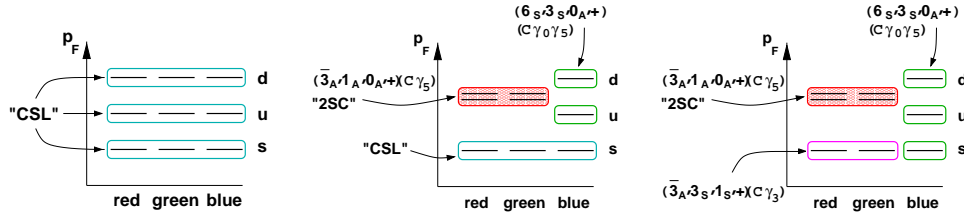


Fig. 4. Pictorial representation of CSL pairing, 2SC + CSL pairing, and 2SC + 1SC pairing in neutral quark matter. See Ref. 75.

modating the tendency for the Fermi momenta to separate is to allow Cooper pairs with nonzero total momentum yielding pairing over parts of the Fermi surfaces. We describe this phase extensively in Section 3. As we will discuss there, this phase may resolve the gCFL phase's stability problems.

2.8. Single-flavor pairing

At densities that are so low that M_s puts such a significant stress on the pairing pattern that even the crystalline phase becomes unfavored, we expect a transition to a phase with no cross-species pairing at all. (This regime will only arise if μ_0 is so small that very large values of $M_s^2 = (\mu_0)$ can arise without being taken so small that nuclear matter becomes favored.)

"Unpaired" quark matter. In most NJL studies, matter with no cross-species pairing at all is described as "unpaired" quark matter. However, it is well known that there are attractive channels for a single-flavor pairing, although they are much weaker than the 2SC and CFL channels.^{26,27,28,29,30} Calculations using NJL models and single-gluon exchange agree that the favored phase in this case is the color-spin-locked (CSL) phase,²⁶ in which all three colors of each flavor, with each pair of colors correlated with a particular direction for the spin. This phase does not break rotational symmetry. See first panel of Fig. 4.

"Unpaired" species in 2SC quark matter.

If the stress is large enough to destroy CFL pairing, and furthermore is large enough to preclude cross-species pairing in which the Cooper pairs have nonzero momentum and form a crystalline color superconducting phase, we can ask whether there is any pattern of BCS pairing which can persist in neutral quark matter with arbitrarily large splitting between Fermi surfaces. The answer to this is no, as demonstrated via an exhaustive search in Ref. 60. Although unlikely, it remains a possibility that up and down quarks with two colors could pair in the 2SC pattern. This does not happen in NJL models in which M_s is a parameter. However, in models in which one instead solves self-consistently for the quark masses, the 2SC phase tends to become more robust. It remains to be seen whether this relative strengthening of the 2SC phase in such models is sufficient to allow it to exist at values of $M_s^2 =$ which are larger than those where the crystalline phases shown in

Fig. 2 and discussed at length in Section 3 are favored.

If there is a regime in which the 2SC phase survives, this leaves the blue quarks unpaired. In that case one might expect a "2SC + CSL" pattern, illustrated in the second panel of Fig. 4, which would again be rotationally symmetric. However, the 2SC pattern breaks the color symmetry, and in order to maintain color neutrality, a color chemical potential is generated, which also affects the unpaired strange quarks, splitting the Fermi momentum of the blue strange quarks away from that of the red and green strange quarks. This is a small effect, but so is the CSL pairing gap, and NJL model calculations indicate that the color chemical potential typically destroys CSL pairing of the strange quarks.⁷⁵ The system falls back on the next best alternative, which is spin-1 pairing of the red and green strange quarks (third panel of Fig. 4).

Single-flavor pairing phases have much lower critical temperatures than multi-flavor phases like the CFL or crystalline phases, perhaps as large as a few MeV, more typically in the eV to many keV range^{26;27;28;29;30}, so they are expected to play a role late in the life of a neutron star.

2.9. Mixed Phases

Another way for a system to deal with a stress on its pairing pattern is phase separation. In the context of quark matter this corresponds to relaxing the requirement of local charge neutrality, and requiring neutrality only over long distances, so we allow a mixture of a positively charged and a negatively charged phase, with a common pressure and a common value of the electron chemical potential μ_e that is not equal to the neutrality value for either phase. Such a mixture of nuclear and CFL quark matter was studied in Ref. 76. In three-flavor quark matter it has been found that as long as we require local color neutrality such mixed phases are not the favored response to the stress imposed by the strange quark mass.^{4;5;42} Phases involving color charge separation have been studied³⁶ but it seems likely that the energy cost of the color-electric fields will disfavor them.

3. The crystallography of three-flavor quark matter

In this section we review recent work by Rajagopal and Sharma.⁵² Here, we focus on explaining the context, the model, the results and the implications. We do not describe the calculations.

3.1. Introduction and context

The investigation of crystalline color superconductivity in three-flavor QCD was initiated in Ref. 69. Although such phases seem to be free from magnetic instability,⁷⁰ it remains to be determined whether such a phase can have a lower free energy than the meson current phase, making it a possible resolution to the gCFL instability. The simplest "crystal" structures do not suffice,^{69;71} but experience in

the two-flavor context⁶⁵ suggests that realistic crystal structures constructed from more plane waves will prove to be qualitatively more robust. The results of Ref. 52 confirm this expectation.

Determining the favored crystal structure(s) in the crystalline color superconducting phase(s) of three-flavor QCD requires determining the gaps and comparing the free energies for very many candidate structures, as there are even more possibilities than the many that were investigated in the two-flavor context.⁶⁵ As there, we shall make a Ginzburg-Landau approximation. This approximation is controlled if $\Delta_0 \gg \Delta$, where Δ is the gap parameter of the crystalline color superconducting phase itself and Δ_0 is the gap parameter in the CFL phase that would occur if m_s were zero. We shall find that the most favored crystal structures can have Δ/Δ_0 as large as $\Delta/\Delta_0 = 1/2$, meaning that we are pushing the approximation hard and so should not trust it quantitatively. Earlier work on a particularly simple one parameter family of "crystal" structures in three-flavor quark matter,⁷¹ simple enough that the analysis could be done both with and without the Ginzburg-Landau approximation, demonstrates that the approximation works when it should and that, at least for very simple crystal structures, when it breaks down it always underestimates the gap and the condensation energy. Furthermore, the Ginzburg-Landau approximation correctly determines which crystal structure among the one parameter family that we analyzed in Ref. 71 has the largest gap and lowest free energy.

The underlying microscopic theory that we use is an NJL model in which the QCD interaction between quarks is replaced by a point-like four-quark interaction with the quantum numbers of single-gluon exchange, analyzed in mean field theory. This is not a controlled approximation. However, it suffices for our purposes: because this model has attraction in the same channels as in QCD, its high density phase is the CFL phase; and, the Fermi surface splitting effects whose qualitative consequences we wish to study can all be built into the model. Note that we shall assume throughout that $\Delta_0 \gg \Delta$. This weak coupling assumption means that the pairing is dominated by modes near the Fermi surfaces. Quantitatively, this means that results for the gaps and condensation energies of candidate crystalline phases are independent of the cutoff in the NJL model when expressed in terms of the CFL gap Δ_0 : if the cutoff is changed with the NJL coupling constant adjusted so that Δ_0 stays fixed, the gaps and condensation energies for the candidate crystalline phases also stay fixed. This makes the NJL model valuable for making the comparisons that are our goal.

We shall consider crystal structures in which there are two condensates

$$\begin{aligned} \text{hudi} &= \frac{1}{3} \sum_a \exp(2iq_3^a \cdot r) \\ \text{husi} &= \frac{1}{2} \sum_a \exp(2iq_2^a \cdot r) : \end{aligned} \quad (3)$$

As in Refs. 69, 71, we neglect hdsi pairing because the d and s Fermi surfaces are twice as far apart from each other as each is from the intervening u Fermi surface.

Were we to set μ_2 to zero, treating only diquark pairing, we would recover the two-flavor Ginzburg-Landau analysis of Ref. 65. There, it was found that the best choice of crystal structure was one in which pairing occurs for a set of eight q_3^a 's pointing at the corners of a cube in momentum space, yielding a condensate with face-centered cubic symmetry. The analyses of three-flavor crystalline color superconductivity in Refs. 69, 71 introduced nonzero μ_2 , but made the simplifying ansatz that pairing occurs only for a single q_3 and a single q_2 . We consider crystal structures with up to eight q_3^a 's and up to eight q_2^a 's.

We evaluate the free energy $\mathcal{F}(\mu_2; \mu_3)$ for each three-flavor crystal structure in a Ginzburg-Landau expansion in powers of the μ 's. We work to order $\mu_2^p \mu_3^q$ with $p + q = 6$. At sextic order, we find that $\mathcal{F}(\mu_2; \mu_3)$ is positive for large μ_2 for all the crystal structures that we investigate.⁵² This is in marked contrast to the result that many two-flavor crystal structures have negative sextic terms, with free energies that are unbounded from below when the Ginzburg-Landau expansion is stopped at sextic order.⁶⁵ Because we find positive sextic terms, we are able to use our sextic Ginzburg-Landau expansion to evaluate \mathcal{F} and $\mathcal{F}(\mu_2; \mu_3)$ for all the structures that we analyze.

We can then identify the two most favorable crystal structures, 2Cube45z and CubeX, which are described further in Section 3.6. To a large degree, our argument that these two structures are the most favorable relies only on two qualitative factors, which we explain in Section 3.5. CubeX and 2Cube45z have gap parameters that are large: a third to a half of μ_0 . We have already discussed the implications of this for the Ginzburg-Landau approximation in Section 3.1 above. The large gaps naturally lead to large condensation energies, easily 1/3 to 1/2 of that in the CFL phase with $M_s = 0$, which is $3 \mu_0^2/2 = \mu_0^2$. This is remarkable, given the only quarks that pair are those lying on (admittedly many) rings on the Fermi surfaces, whereas in the CFL phase with $M_s = 0$ pairing occurs over the entire u, d and s Fermi surfaces. The gapless CFL (gCFL) phase provides a useful comparison at nonzero M_s . For $2 \mu_0 < M_s^2 < 5/2 \mu_0$, model analyses that are restricted to isotropic phases predict a gCFL phase,^{4;5;44} finding this phase to have lower free energy than either the CFL phase or unpaired quark matter, as shown in Fig. 2. However, this phase is unstable to the formation of current-carrying condensates.^{7;8;9;10;11;12;13;14;15;16;17;18} and so it cannot be the ground state. The true ground state must have lower free energy than that of the gCFL phase, and for this reason the gCFL free energy provides a useful benchmark. We find that three-flavor crystalline color superconducting quark matter with one or other of the two crystal structures that we argue are most favorable has lower free energy (greater condensation energy) than CFL quark matter, gCFL quark matter, and unpaired quark matter for

$$2.9 \mu_0 < \frac{M_s^2}{\mu_0} < 10.4 \mu_0 : \quad (4)$$

(See Fig. 2 above.) This window in parameter space is in no sense narrow. Our

results therefore indicate that three-flavor crystalline quark matter will occur over a wide range of densities. (That is unless the pairing between quarks is so strong, i.e. μ_0 so large making $M_s^2 = \mu_0$ so small, that quark matter is in the CFL phase all the way down to the density at which quark matter is superseded by nuclear matter.) However, our results also indicate that unless the Ginzburg-Landau approximation is underestimating the condensation energy of the crystalline phase by about a factor of two, there is a fraction of the "gCFL window" (with $2\mu_0 < M_s^2 < 2.9\mu_0$, in the Ginzburg-Landau approximation) in which no crystalline phase has lower free energy than the gCFL phase. This is thus the most likely regime in which to find the current-carrying meson condensates of Refs. 14, 18.

3.2. Model, simplifications and ansatz

3.2.1. Neutral unpaired three-flavor quark matter

The analysis of beta-equilibrated neutral three-flavor quark matter in an NJL model has been discussed in detail elsewhere (For example, Ref. 5), and here we just summarize the main points. We assume that the up and down quarks are massless. The strange quark mass is a parameter M_s . We couple a chemical potential μ to quark number, and always work at $\mu = 500$ MeV. To ensure neutrality under color and electromagnetism we couple a chemical (electrostatic) potential μ_e to negative electric charge, and chemical (color-electrostatic) potentials μ_3 and μ_8 to the diagonal generators of $SU(3)_{\text{color}}$. In full QCD these gauged chemical potentials would be the zeroth components of the corresponding gauge fields, and would naturally be forced to their neutrality values.^{33,77} In the NJL context, we enforce neutrality explicitly by choosing them to satisfy the neutrality conditions $\frac{\mu}{\mu_e} = \frac{\mu}{\mu_3} = \frac{\mu}{\mu_8} = 0$. The assumption of beta-equilibrium is built into the calculation via the fact that the only flavor-dependent chemical potential we introduce is μ_e , ensuring for example that the chemical potentials of d and s quarks with the same color must be equal.

The presence of a nonzero strange quark mass, combined with the requirements of equilibrium under weak interactions and charge neutrality, drives down the number of strange quarks, and introduces electrons and additional down quarks. We assume that this is a small effect, i.e. we expand in powers of $\mu_e = \mu$ and $M_s^2 = \mu^2$. Working to linear order, we can simply treat the strange quark mass as a shift of

$M_s^2 = (2\mu)$ in the strange quark chemical potential. (The corrections from higher-order terms in $M_s^2 = \mu^2$ in an NJL analysis of a two-flavor crystalline color superconductor have been evaluated and found to be small,⁶⁴ and we expect the same to be true here.) In this approximation we find the Fermi momenta of the quarks and electrons are given by

$$\begin{aligned} p_F^d &= \mu + \frac{\mu_e}{3} & p_F^u &= \mu - \frac{2\mu_e}{3} & p_F^e &= \mu_e \\ p_F^s &= \mu + \frac{\mu_e}{3} + \frac{M_s^2}{2} & & & & \end{aligned} \quad (5)$$

and their free energy is

$$\begin{aligned} \text{unpaired} = & \frac{3(p_F^u)^4 + 3(p_F^d)^4 + (p_F^e)^4}{12\pi^2} + \frac{3}{2} \int_0^{p_F^s} p^2 dp \sqrt{p^2 + M_s^2} - \frac{e}{3} \\ & \frac{3}{4\pi^2} \mu^4 + \frac{1}{2\pi^2} M_s^2 e - \frac{1}{2} \mu_e^2 + \dots \end{aligned} \quad (6)$$

To this order, electric neutrality requires

$$e = \frac{M_s^2}{4}; \quad (7)$$

and because we are working to lowest order in $M_s^2 = \mu^2$ we need no longer be careful about the distinction between p_F 's and μ 's, as we can simply think of the three flavors of quarks as if they have chemical potentials

$$\begin{aligned} \mu_d &= \mu_u + 2\mu_3 \\ \mu_u &= p_F^u \\ \mu_s &= \mu_u - 2\mu_2 \end{aligned} \quad (8)$$

where, using (7), $p_F^u = \frac{M_s}{6}$ and

$$\mu_3 = \mu_2 = \frac{M_s^2}{8}; \quad (9)$$

with the choice of subscripts indicating that $2\mu_2$ is the splitting between the Fermi surfaces for quarks 1 and 3 and $2\mu_3$ is that between the Fermi surfaces for quarks 1 and 2, identifying u;d;s with 1;2;3.

3.2.2. BCS pairing and neutrality

BCS pairing introduces qualitative changes into the analysis of neutrality.^{51;33;34;4} For example, in the CFL phase $\mu_e = 0$ and μ_8 is nonzero and of order $M_s^2 = \mu^2$. This arises because the construction of a phase in which BCS pairing occurs between fermions whose Fermi surface would be split in the absence of pairing can be described as follows. First, adjust the Fermi surfaces of those fermions that pair to make them equal. This costs a free energy price of order μ^2 . And, it changes the relation between the chemical potentials and the particle numbers, meaning that the μ 's required for neutrality can change qualitatively as happens in the CFL example. Second, pair. This yields a free energy benefit of order μ_0^2 , where μ_0 is the gap parameter describing the BCS pairing. Hence, BCS pairing will only occur if the attraction between the fermions is large enough that $\mu_0 \gg \mu$. In the CFL context, in which u , d , s and h pairing is fighting against the splitting between the d , u and s Fermi surfaces described above, it turns out that CFL pairing can occur if $\mu_0 > 4\mu = M_s^2 = (2\mu)^2$,⁴ a criterion that is reduced somewhat by kaon condensation which acts to stabilize CFL pairing.^{38;41}

We are now considering quark matter at densities that are low enough ($\mu < M_s^2 = (2\mu_0)^2$) that CFL pairing is not possible. The gap parameter μ_0 that would

characterize the CFL phase if M_s^2 and μ were zero is nevertheless an important scale in our problem, as it quantifies the strength of the attraction between quarks. Estimates of the magnitude of μ_0 are typically in the tens of MeV, perhaps as large as 100 MeV.³ We shall treat μ_0 as a parameter, and quote results for $\mu_0 = 25$ MeV, although our results can easily be scaled to any value of μ_0 as long as the weak-coupling approximation $\mu_0 \ll \Lambda$ is respected.⁵²

3.2.3. Crystalline color superconductivity in two-flavor quark matter

Crystalline color superconductivity can be thought of as the answer to the question: "Is there a way to pair quarks at differing Fermi surfaces without first equalizing their Fermi momenta, given that doing so exacts a cost?" The answer is "Yes, but it requires Cooper pairs with nonzero total momentum." Ordinary BCS pairing pairs quarks with momenta p and $-p$, meaning that if the Fermi surfaces are split at most one member of a pair can be at its Fermi surface. In the crystalline color superconducting phase, pairs with total momentum $2q$ condense, meaning that one member of the pair has momentum $p + q$ and the other has momentum $-p + q$ for some p .^{72;19} Suppose for a moment that only u and d quarks pair, making the analyses of a two-flavor model found in Refs. 19, 61, 62, 63, 64, 65, 66, 67, 68 (and really going back to Ref. 72) valid. We sketch the results of this analysis in this subsection.

The simplest "crystalline" phase is one in which only pairs with a single q condense, yielding a condensate

$$\psi_u(x) \psi_d(x) i / \exp(2iq \cdot r) \quad (10)$$

that is modulated in space like a plane wave. (Here and throughout, we shall denote by r the spatial three-vector corresponding to the Lorentz four-vector x .) Assuming that $\mu_0 \ll \Lambda$, the energetically favored value of $|q|$ turns out to be $q = \mu_0 / \Lambda$, where the proportionality constant is given by $\mu_0 / \Lambda = 1.1997$.^{72;19} If μ_0 / Λ were 1, then the only choice of p for which a Cooper pair with momentum $(-p + q; p + q)$ would describe two quarks each on their respective Fermi surfaces would correspond to a quark on the north pole of one Fermi surface and a quark on the south pole of the other. Instead, with $\mu_0 / \Lambda > 1$, the quarks on each Fermi surface that can pair lie on one ring on each Fermi surface, the rings having opening angle $2 \cos^{-1}(1 - \mu_0 / \Lambda) = 67.1^\circ$. The energetic calculation that determines μ_0 / Λ can be thought of as balancing the gain in pairing energy as μ_0 / Λ is increased beyond 1, allowing quarks on larger rings to pair, against the kinetic energy cost of Cooper pairs with greater total momentum. If the $\mu_0 \rightarrow 0$ Ginzburg-Landau limit is not assumed, the pairing rings change from circular lines on the Fermi surfaces into ribbons of thickness $\sim \mu_0 / \Lambda$ and angular extent $\sim \mu_0 / \Lambda$.

After solving a gap equation for μ_0 / Λ and then evaluating the free energy of the phase with condensate (10), one finds that this simplest "crystalline" phase is favored over two-flavor quark matter with either no pairing or BCS pairing only within

a narrow window

$$0.707 \mu_{2SC} < \mu < 0.754 \mu_{2SC}; \quad (11)$$

where μ_{2SC} is the gap parameter for the two-flavor phase with 2SC (2-flavor, 2-color) BCS pairing found at $\mu = 0$. At the upper boundary of this window, $\mu \neq 0$ and one finds a second order phase transition between the crystalline and unpaired phases. At the lower boundary, there is a first order transition between the crystalline and BCS paired phases. The crystalline phase persists in the weak coupling limit only if $\mu = \mu_{2SC}$ is held fixed, within the window (11), while the standard weak-coupling limit $\mu_{2SC} = 0$ is taken. Looking ahead to our context, and recalling that in three-flavor quark matter $\mu = M_s^2/(8\pi)$, we see that at high densities one finds the CFL phase (which is the three-flavor quark matter BCS phase) and in some window of lower densities one finds a crystalline phase. In the vicinity of the second order transition, where $\mu \neq 0$ and in particular where $\mu = 0$ and, consequently given (11), $\mu = \mu_{2SC} = 0$ a Ginzburg-Landau expansion of the free energy order by order in powers of μ is controlled.

The Ginzburg-Landau analysis can then be applied to more complicated crystal structures in which Cooper pairs with several different q 's, all with the same length but pointing in different directions, arise.⁶⁵ This analysis indicates that a face-centered cubic structure constructed as the sum of eight plane waves with q 's pointing at the corners of a cube is favored, but it does not permit a quantitative evaluation of μ . The Ginzburg-Landau expansion of the free energy has terms that are quartic and sextic in μ whose coefficients are both large in magnitude and negative. To this order, μ is not bounded from below. This means that the Ginzburg-Landau analysis predicts a strong first order phase transition between the crystalline and unpaired phase, at some μ significantly larger than $0.754 \mu_{2SC}$, meaning that the crystalline phase occurs over a range of μ that is much wider than (11), but it precludes the quantitative evaluation of the μ at which the transition occurs, of μ , or of μ .

In three-flavor quark matter, all the crystalline phases analyzed in Ref. 52 have Ginzburg-Landau free energies with positive sextic coefficient, meaning that they can be used to evaluate μ , and the location of the transition from unpaired quark matter to the crystalline phase with a postulated crystal structure. For the most favored crystal structures, we shall see that the window in parameter space in which they occur is given by (4), which is in no sense narrow.

3.2.4. Crystalline color superconductivity in neutral three-flavor quark matter

We now turn to three-flavor crystalline color superconductivity. We shall make weak coupling (namely μ_0 ; μ_0) and Ginzburg-Landau (namely μ_0 ; μ_0) approximations throughout. The analysis of neutrality in three-flavor quark matter in a crystalline color superconducting phase is very simple in the Ginzburg-Landau limit in which μ_0 : because the construction of this phase does not involve

rearranging any Fermion momenta prior to pairing, and because the assumption

implies that the pairing does not significantly change any number densities, neutrality is achieved with the same chemical potentials $\mu_e = \mu_s = 4$ and $\mu_3 = \mu_8 = 0$ as in unpaired quark matter, and with Fermion momenta given in Eqs. (5) and (8) as in unpaired quark matter.

We consider a condensate of the form

$$\chi_{ij}(\mathbf{x}) C_{5j}(\mathbf{x}) i / \sum_{I=1}^3 \sum_{\mathbf{q}_I} e^{2i\mathbf{q}_I \cdot \mathbf{r}} \chi_{Iij}; \quad (12)$$

where i, j are color indices, i, j are flavor indices, and where $\mathbf{q}_1^a, \mathbf{q}_2^a$ and \mathbf{q}_3^a and $\mathbf{q}_1, \mathbf{q}_2$ and \mathbf{q}_3 are the wave vectors and gap parameters describing pairing between the (d;s), (u;s) and (u;d) quarks respectively, whose Fermion momenta are split by $2\mathbf{q}_1, 2\mathbf{q}_2$ and $2\mathbf{q}_3$ respectively. From (8), we see that $\mathbf{q}_2 = \mathbf{q}_3 = \mathbf{q}_1 = 2\mathbf{M}_s = (8)$. For each I , \mathbf{q}_I is a set of momentum vectors that define the periodic spatial modulation of the crystalline condensate describing pairing between the quarks whose flavor is not I , and whose color is not I . Our goal in this paper is to compare condensates with different choices of \mathbf{q}_I 's, that is with different crystal structures. To shorten expressions, we will henceforth write $\mathbf{q}_I^a = \mathbf{q}_I^a 2\mathbf{f}_{\mathbf{q}_I}$. The condensate (12) has the color-flavor structure of the CFL condensate (obtained by setting all \mathbf{q}_I 's to zero) and is the natural generalization to nontrivial crystal structures of the condensate previously analyzed in Refs. 69, 71, in which each \mathbf{q}_I contained only a single vector.

In all our results, although not in the derivation of the Ginzburg-Landau approximation itself in Ref. 52, we shall make the further simplifying assumption that $\mu_1 = 0$. Given that μ_1 is twice μ_2 or μ_3 , it seems reasonable that $\mu_1 = 2\mu_2; 2\mu_3$. We leave a quantitative investigation of condensates with $\mu_1 \neq 0$ to future work.

3.2.5. NJL Model and Mean-Field Approximation

As discussed in Section 3.1, we shall work in a NJL model in which the quarks interact via a point-like four-quark interaction, with the quantum numbers of single-gluon exchange, analyzed in mean field theory. By this we mean that the interaction term is

$$\mathcal{L}_{\text{interaction}} = \frac{3}{8} (\bar{\psi}^A)(\psi^A)(\bar{\psi}^A)(\psi^A); \quad (13)$$

The full expression for $\bar{\psi}^A$ is $(\bar{\psi}^A)_{ij} = (\bar{\psi}^A)_{ij}$, where the T^A are the color Gell-Mann matrices. The NJL coupling constant has dimension -2 , meaning that an ultraviolet cutoff must be introduced as a second parameter in order to fully specify the interaction. Defining as the restriction that momentum integrals be restricted to a shell around the Fermi surface, $\mu < p < \mu + \Lambda$, the CFL gap parameter can then be evaluated:^{3,65}

$$\mu_0 = 2^{\frac{2}{3}} \exp \left(-\frac{2}{\Lambda^2} \right) : \quad (14)$$

In the limit in which $\mu \gg m_q$, all our results can be expressed in terms of μ ; neither m_q nor Λ appear.⁵² This reflects the fact that in this limit the physics of interest is dominated by quarks near the Fermi surfaces, not near Λ , and so once μ is used as the parameter describing the strength of the attraction between quarks, Λ is no longer visible; the cutoff only appears in the relation between μ and Λ , not in any comparison among different possible paired phases. In our numerical evaluations, we shall take $\mu = 500 \text{ MeV}$, $\Lambda = 100 \text{ MeV}$, and adjust G to be such that μ is 25 MeV.

In the mean-field approximation, the interaction Lagrangian (13) takes the form

$$\mathcal{L}_{\text{interaction}} = \frac{1}{2} (\bar{\psi})^T + \frac{1}{2} \bar{\psi}^T (\psi); \quad (15)$$

where ψ is related to the diquark condensate by the relations

$$\psi = \frac{3}{4} \Lambda^{\text{A}} h^{\text{T}} i(\Lambda^{\text{A}})^{\text{T}}; \quad (16)$$

The ansatz (12) can now be made precise: we take

$$\psi = C_F(\psi) C^{-5}; \quad (17)$$

with

$$C_F(\psi)_{ij} = \sum_{I=1}^{X^3} \sum_{q_I^a} X_I e^{2iq_I^a \cdot r_I} \psi_{Iij}; \quad (18)$$

Upon making the mean-field approximation, the full Lagrangian is quadratic and can be written simply upon introducing two component Nambu-Gorkov spinors. Upon so doing, gap equations can easily be derived.⁵² Without further approximation, however, they are not tractable because without further approximation it is not consistent to choose finite sets $f_{q_I g}$. When several plane waves are present in the condensate, they induce an infinite tower of higher momentum condensates.⁶⁵ The reason why the Ginzburg-Landau approximation, to which we now turn, is such a simplification is that it eliminates these higher harmonics.

3.3. Ginzburg-Landau Approximation

The form of the Ginzburg-Landau expansion of the free energy can be derived using only general arguments.

We shall only consider crystal structures in which all the vectors q_I^a in the crystal structure $f_{q_I g}$ are "equivalent". By this we mean that a rigid rotation of the crystal structure can be found which maps any q_I^a to any other q_I^b leaving the set $f_{q_I g}$ invariant. (If we did not make this simplifying assumption, we would need to introduce different gap parameters Δ_I^a for each vector in $f_{q_I g}$.) As explained in Section 3.2.4, the chemical potentials that maintain neutrality in three-flavor

crystalline color superconducting quark matter are the same as those in neutral unpaired three-flavor quark matter. Therefore,

$$\epsilon_{\text{crystalline}} = \epsilon_{\text{unpaired}} + \epsilon(\mu_1; \mu_2; \mu_3); \quad (19)$$

with $\epsilon_{\text{unpaired}}$ given in (6) with (7), and with $\epsilon(0;0;0) = 0$. Our task is to evaluate the condensation energy $\epsilon(\mu_1; \mu_2; \mu_3)$. Since our Lagrangian is baryon number conserving and contains no weak interactions, it is invariant under a global $U(1)$ symmetry for each flavor. This means that ϵ must be invariant under $\mu_I \rightarrow \mu_I + e^{i\theta_I}$ for each I , meaning that each of the three μ_I 's can only appear in the combination μ_I^3 . (Of course, the ground state can and does break these $U(1)$ symmetries spontaneously; what we need in the argument we are making here is only that they are not explicitly broken in the Lagrangian.) We conclude that if we expand $\epsilon(\mu_1; \mu_2; \mu_3)$ in powers of the μ_I 's up to sextic order, it must take the form

$$\begin{aligned} \epsilon(\mu_1; \mu_2; \mu_3) = & \frac{2}{2} \sum_I \mu_I^2 P_I + \frac{1}{2} \sum_I \mu_I^4 \left(\mu_I^2 \right)^2 + \sum_{I>J} \mu_I \mu_J \mu_I \mu_J \mu_I \mu_J \\ & + \frac{1}{3} \sum_I \mu_I^6 + \sum_{I \neq J} \mu_I \mu_J \mu_I \mu_J \mu_I \mu_J \mu_I \mu_J + \mu_{123} \mu_1 \mu_1 \mu_2 \mu_2 \mu_3 \mu_3; \end{aligned} \quad (20)$$

where we have made various notational choices for convenience. The overall prefactor of $2^{-2} = 2^{-2}$ is the density of states at the Fermi surface of unpaired quark matter with $M_s = 0$; it is convenient to define all the coefficients in the Ginzburg-Landau expansion of the free energy relative to this. We have defined $P_I = \dim f_{q_I g}$, the number of plane waves in the crystal structure for the condensate describing pairing between quarks whose flavor and color are not I . Writing the prefactor P_I multiplying the quadratic term and writing the factors of $\frac{1}{2}$ and $\frac{1}{3}$ multiplying the quartic and sextic terms ensures that the μ_I^2 , μ_I^4 and μ_I^6 coefficients are defined the same way as in Ref. 65. The form of the Ginzburg-Landau expansion (20) is model independent, whereas the expressions for the coefficients P_I , μ_I , μ_J , $\mu_I \mu_J$ and μ_{123} for a given ansatz for the crystal structure are model-dependent. In Sections IV and V of Ref. 52 these coefficients are evaluated by deriving the Ginzburg-Landau approximation to this model.

We see in Eq. (20) that there are some coefficients — namely μ_I , μ_I and μ_I — which multiply polynomials involving only a single μ_I . Suppose that we keep a single μ_I nonzero, setting the other two to zero. This reduces the problem to one with two-flavor pairing only, and the Ginzburg-Landau coefficients for this problem have been calculated for many different crystal structures in Ref. 65. We can then immediately use these coefficients, called μ_I , μ_I and μ_I in Ref. 65, to determine our μ_I , μ_I and μ_I . Using μ_I as an example, we conclude that

$$\mu_I = \epsilon(\mu_I; \mu_I) = -1 + \frac{\mu_I}{2q_I} \log \frac{q_I + \mu_I}{q_I - \mu_I} - \frac{1}{2} \log \frac{\frac{2}{2sc}}{4(q_I^2 - \frac{2}{I})}; \quad (21)$$

where ϵ_I is the splitting between the Fermi surfaces of the quarks with the two flavors other than I and $q_I = |\mathbf{q}_I|$ is the length of the \mathbf{q} -vectors in the set $\{q_I\}$. (We shall see momentarily why all have the same length.) In (21), μ_{2SC} is the gap parameter in the BCS state obtained with $\epsilon_I = 0$ and ϵ_I nonzero with the other two gap parameters set to zero. Assuming that $\mu_0 = 0$, this gap parameter for 2SC (2-flavor, 2-color) BCS pairing is given by^{21;3}

$$\mu_{2SC} = 2^{\frac{1}{3}} \mu_0 : \quad (22)$$

In the Ginzburg-Landau approximation, in which the ϵ_I are assumed to be small, we must first minimize the quadratic contribution to the free energy, before proceeding to investigate the consequences of the quartic and sextic contributions. Notice that ϵ_I depends on the cutoff and the NJL coupling constant only through μ_{2SC} , and depends only on the ratios $q_I = \epsilon_I$ and $\epsilon_I = \mu_{2SC}$. ϵ_I is negative for $\epsilon_I = \mu_{2SC} < 0.754$, and for a given value of this ratio for which $\epsilon_I < 0$, ϵ_I is most negative and (21) is minimized for^{72;19;65}

$$q_I = \epsilon_I \text{ with } \epsilon_I = 1.1997 ; \quad (23)$$

where ϵ_I is defined as the solution to

$$\frac{1}{2} \log \frac{\epsilon_I + 1}{\epsilon_I - 1} = 1 : \quad (24)$$

We therefore set $q_I = \epsilon_I$ henceforth and upon so doing find that (21) becomes

$$(\epsilon_I) = \frac{1}{2} \log \frac{\mu_{2SC}^2}{4 \epsilon_I^2 (\epsilon_I^2 - 1)} : \quad (25)$$

Minimizing ϵ_I has fixed the length of all the \mathbf{q} -vectors in the set $\{q_I\}$, thus eliminating the possibility of higher harmonics.

It is helpful to imagine the (three) sets $\{q_I\}$ as representing the vertices of (three) polyhedra in momentum space. By minimizing ϵ_I , we have learned that each polyhedron $\{q_I\}$ can be inscribed in a sphere of radius ϵ_I . From the quadratic contribution to the free energy, we do not learn anything about what shape polyhedra are preferable. In fact, the quadratic analysis in isolation would indicate that if $\epsilon_I < 0$ (which happens for $\epsilon_I < 0.754 \mu_{2SC}$) then modes with arbitrarily many different q_I 's should condense. It is the quartic and sextic coefficients that describe the interaction among the modes, and hence control what shape polyhedra are in fact preferable.

The quartic and sextic coefficients ϵ_I and ϵ_I can also be taken directly from the two-flavor results of Ref. 65. Note that these coefficients are independent of μ_{2SC} and the NJL coupling constant and cutoff, as long as the weak-coupling approximation μ_{2SC} is valid.^{65;52} Given this, and given (23), the only dimensionful quantity on which they can depend is ϵ_I . They are therefore given by $\epsilon_I = \epsilon_I^2$ and $\epsilon_I = \epsilon_I^4$ where ϵ_I and ϵ_I are dimensionless quantities depending only on the directions of the vectors in the set $\{q_I\}$. and have been evaluated for many

crystal structures in Ref. 65, resulting in two qualitative conclusions. Recall that, as reviewed in Section 3.2.3, the presence of a condensate with some \hat{q}_I^a corresponds to pairing on a ring on each Fermi surface with opening angle 67.1° . The first qualitative conclusion is that any crystal structure in which there are two \hat{q}_I^a 's whose pairing rings intersect has very large, positive, values of both β_I and β_{II} , meaning that it is strongly disfavored. The second conclusion is that regular structures, those in which there are many ways of adding four or six \hat{q}_I^a 's to form closed figures in momentum space, are favored. Consequently, the favored crystal structure in the two-avor case has 8 \hat{q}_I^a 's pointing towards the corners of a cube.⁶⁵ Choosing the polyhedron in momentum space to be a cube yields a face-centered cubic modulation of the condensate in position space.

Because the β_I and β_{II} coefficients in our problem can be taken over directly from the two-avor analysis, we can expect that it will be unfavorable for any of the three sets $f_{q_I}g$ to have more than eight vectors, or to have any vectors closer together than 67.1° . It can be proved that β_{IJ} is always positive, and in all cases investigated to date β_{IIJ} also turns out to be positive.⁵² This means that we know of no exceptions to the rule that if a particular $f_{q_I}g$ is unfavorable as a two-avor crystal structure, then any three-avor condensate in which this set of q -vectors describes either the β_1 , β_2 or β_3 crystal structure is also disfavored.

The coefficients β_{IJ} and β_{IIJ} cannot be read off from a two-avor analysis because they multiply terms involving more than one β_I and hence describe the interaction between the three different β_I 's. Before evaluating the expressions for the coefficients,⁵² we make the further simplifying assumption that $\beta_1 = 0$, because the separation β_1 between the d and s Fermi surfaces is twice as large as that between either and the intervening u Fermi surface. This simplifies (20) considerably, eliminating the β_{123} term and all the β_{IJ} and β_{IIJ} terms except β_{32} , β_{223} and β_{332} . We further simplify the problem by focussing on crystal structures for which $f_{\hat{q}_2}g$ and $f_{\hat{q}_3}g$ are "exchange symmetric", meaning that there is a sequence of rigid rotations and reflections which when applied to all the vectors in $f_{\hat{q}_2}g$ and $f_{\hat{q}_3}g$ together has the effect of exchanging $f_{\hat{q}_2}g$ and $f_{\hat{q}_3}g$. If we choose an exchange symmetric crystal structure, upon making the approximation that $\beta_2 = \beta_3$ and restricting our attention to solutions with $\beta_2 = \beta_3$ we have the further simplification that $\beta_{322} = \beta_{233}$.

Upon making these simplifying assumptions, the only dimensionful quantity on which β_{32} and β_{322} can depend is β , meaning that $\beta_{32} = \beta_{32} = \beta^2$ and $\beta_{322} = \beta_{322} = \beta^4$.⁵² Here, β_{32} and β_{322} are dimensionless numbers, depending only on the shape and relative orientation of the polyhedra $f_{\hat{q}_2}g$ and $f_{\hat{q}_3}g$, which must be evaluated for each crystal structure. Doing so requires evaluating one loop Feynman diagram with 4 or 6 insertions of β_I 's. Each insertion of β_I ($-\beta_I$) adds (subtracts) momentum $2q_I^a$ for some a , meaning that the calculation consists of a bookkeeping task (determining which combinations of 4 or 6 q_I^a 's are allowed) that grows rapidly in complexity with the complexity of the crystal structure and a loop integration

that is nontrivial because the momentum in the propagator changes after each insertion. See Ref. 52, where this calculation is carried out explicitly for 11 crystal structures in a mean-field NJL model upon making the weak coupling (g_0 ; μ_0) approximation. Within this approximation, neither the NJL cutoff nor the NJL coupling constant appear in any quartic or higher Ginzburg-Landau coefficient, and they influence only through μ_{2SC}/μ_0 . Hence, the details of the model do not matter as long as one thinks of μ_0 as a parameter, kept fixed.

3.4. General results

Upon assuming that $\mu_1 = 0$, assuming that the crystal structure is exchange symmetric, and making the approximation that $\mu_2 = \mu_3 = M_s^2/(8\mu_0)$, the free energy (20) reduces to

$$\begin{aligned} \mathcal{F}(\mu_2; \mu_3) = & \frac{2}{2} P(\mu_2) \mu_2^2 + \frac{2}{3} \mu_3^2 + \frac{1}{2} \frac{1}{\mu_2^2} (\mu_2^4 + \mu_3^4) + \frac{32}{2} \frac{\mu_2^2 \mu_3^2}{\mu_2^2} \\ & + \frac{1}{3} \frac{1}{\mu_2^4} (\mu_2^6 + \mu_3^6) + \frac{322}{2} (\frac{\mu_2^2}{2} \frac{\mu_3^4}{3} + \frac{\mu_2^4}{2} \frac{\mu_3^2}{3}) ; \end{aligned} \quad (26)$$

where P , μ_2 , μ_3 and μ_{322} are the dimensionless constants that can be calculated for each crystal structure,⁵² and where the μ -dependence of \mathcal{F} is given by Eq. (25). It is easy to show that extrema of $\mathcal{F}(\mu_2; \mu_3)$ in $(\mu_2; \mu_3)$ -space must either have $\mu_2 = \mu_3 = 0$, or have one of μ_2 and μ_3 vanishing.⁵² The latter class of extrema are two-flavor crystalline phases. We are interested in the solutions with $\mu_2 = \mu_3 = 0$. (Furthermore, the three-flavor crystalline phases with $\mu_2 = \mu_3 = 0$ are electrically neutral whereas the two-flavor solutions in which only one of the μ 's is nonzero are not.⁵²) Setting $\mu_2 = \mu_3 = 0$, the free energy becomes

$$\mathcal{F}(0) = \frac{2}{2} P(0) \mu_2^2 + \frac{4}{2} \frac{\mu_2^4}{\mu_2^2} e + \frac{6}{3} \frac{\mu_2^6}{\mu_2^4} e ; \quad (27)$$

where we have defined

$$\begin{aligned} e &= 2 + \mu_{32} \\ e &= 2 + 2\mu_{322} ; \end{aligned} \quad (28)$$

We have arrived at a familiar-looking sextic order Ginzburg-Landau free energy function, whose coefficients can be evaluated for specific crystal structures.⁵²

If e and e are both positive, the free energy (27) describes a second order phase transition between the crystalline color superconducting phase and the normal phase at the μ at which $\mathcal{F}(\mu)$ changes sign. From (25), this critical point occurs where $\mu = 0.754 \mu_{2SC}$. In plotting our results, we will take the CFL gap to be $\mu_0 = 25 \text{ MeV}$, making $\mu_{2SC} = 2^{1/3} \mu_0 = 31.5 \text{ MeV}$. Recalling that $\mu_s^2 = (8\mu_0)$, this puts the second order phase transition at

$$\begin{aligned} \frac{M_s^2}{\mu_0} &= 6.03 \mu_{2SC} = 7.60 \mu_0 = 190.0 \text{ MeV} ; \\ &= 0 \end{aligned} \quad (29)$$

(The authors of Refs. 69, 71 neglected to notice that it is μ_{2SC} , rather than the CFL gap μ_0 , that occurs in Eqs. (21) and (25) and therefore controls the μ at which $\mu = 0$. In analyzing the crystalline phase in isolation, this is immaterial since either μ_0 or μ_{2SC} could be taken as the parameter defining the strength of the interaction between quarks. However, we shall compare the free energies of the CFL, gCFL and crystalline phases, and in making this comparison it is important to take into account that $\mu_{2SC} = 2^{1/3} \mu_0$.) For values of $M_s^2 =$ that are smaller than (29) (that is, lower densities), $\mu < 0$ and the free energy is minimized by a nonzero μ_{min} and thus describes a crystalline color superconducting phase.

If $\mu_e < 0$ and $\mu_e > 0$, then the free energy (27) describes a first order phase transition between unpaired and crystalline quark matter occurring at $\mu = \mu_c = 3 \mu_e^2 = (32 P_e)$. At this positive value of μ , the function $\mu(\mu)$ has a minimum at $\mu = 0$ with $\mu = 0$, initially rises quadratically with increasing μ , and is then turned back downward by the negative quartic term before being turned back upwards again by the positive sextic term, yielding a second minimum at

$$\mu_c = \frac{3 \mu_e^2}{4 \mu_e}; \quad (30)$$

also with $\mu = 0$, which describes a crystalline color superconducting phase. For $\mu_e < 0$, the crystalline phase is favored over unpaired quark matter. Eq. (25) determines the value of μ_c , and hence $M_s^2 =$, at which $\mu = \mu_c$ and the first order phase transition occurs. If $\mu_e > 0$, the transition occurs at a value of $M_s^2 =$ that is greater than (29) by a factor $(1 + \mu_e)$. See Fig. 7 in Section 3.7 for an explicit example of plots of μ versus M_s^2 for various values of μ_e for one of the crystal structures that we describe.

A necessary condition for the Ginzburg-Landau approximation to be quantitatively reliable is that the sextic term in the free energy is small in magnitude compared to the quartic, meaning that $\mu^2 \mu_e^2 = \mu_e^2$. If the transition between the unpaired and crystalline phases is second order, then this condition is satisfied close enough to the transition where $\mu \neq 0$. However, if $\mu_e < 0$ and $\mu_e > 0$, making the transition first order, we see from (30) that at the first order transition itself μ is large enough to make the quantitative application of the Ginzburg-Landau approximation marginal. This is a familiar result, coming about whenever a Ginzburg-Landau approximation predicts a first order phase transition because at the first order phase transition the quartic and sextic terms are balanced against each other. We shall find that our Ginzburg-Landau analysis predicts a first order phase transition; knowing that it is therefore at the edge of its quantitative reliability, we shall focus on qualitative conclusions.

3.5. Two plane wave structure

We begin with the simplest three-flavor "crystal" structure in which f_{q_2g} and f_{q_3g} each contain only a single vector, yielding a condensate in which the u and

hudi condensates are each plane waves. This simple condensate yields a qualitative lesson which proves extremely helpful in winnowing the space of multiple plane wave crystal structures.⁵²

For this simple "crystal" structure, all the coefficients in the Ginzburg-Landau free energy can be evaluated analytically.⁵² The terms that occur in the three-flavor case but not in the two-flavor case, namely κ_{32} and κ_{322} , describe the interaction between the two condensates and hence depend on the angle between q_2 and q_3 . For any angle θ , both κ_{32} and κ_{322} are positive, both increase monotonically with θ , and both diverge as $\theta \rightarrow \pi$.⁵² This tells us that within this two plane wave ansatz, the most favorable orientation is $\theta = 0$, namely $q_2 \parallel q_3$. Making this choice yields the smallest possible ϵ_c and ϵ_c within this ansatz, and hence the largest possible μ and condensation energy, again within this ansatz. The divergence at $\theta = \pi$ tells us that choosing q_2 and q_3 precisely antiparallel exacts an infinite free energy price in the combined Ginzburg-Landau and weak-coupling limit in which $\mu \rightarrow 0$, meaning that in this limit if we chose $\theta = \pi$ we find $\mu = 0$. Away from the Ginzburg-Landau limit, when the pairing rings on the Fermi surfaces widen into bands, choosing $\theta = \pi$ exacts a finite price meaning that μ is nonzero but smaller than that for any other choice of θ .

The high cost of choosing q_2 and q_3 precisely antiparallel can be understood qualitatively as arising from the fact that in this case the ring of states on the u-quark Fermi surface that "want to" pair with d-quarks coincides precisely with the ring that "wants to" pair with s-quarks.⁷¹ The simple two plane wave ansatz has been analyzed in the same NJL model that we employ upon making the weak-coupling approximation but without making a Ginzburg-Landau approximation.⁷¹ All the qualitative lessons that we have learned from the Ginzburg-Landau approximation remain valid, including the favorability of the choice $\theta = 0$, but we learn further that in the two plane wave case the Ginzburg-Landau approximation always underestimates μ .⁷¹

The analysis of the simple two plane wave "crystal" structure, together with the observation that in more complicated crystal structures with more than one vector in $f_{q_2}g$ and $f_{q_3}g$ the Ginzburg-Landau coefficient κ_{32} (κ_{322}) is given in whole (in part) by a sum of many two plane wave contributions, yields an important lesson for how to construct favorable crystal structures for three-flavor crystalline color superconductivity:⁵² $f_{q_2}g$ and $f_{q_3}g$ should be rotated with respect to each other in a way that best keeps vectors in one set away from the antipodes of vectors in the other set. Crystal structures in which any of the vectors in $f_{q_2}g$ are close to antiparallel to any of the vectors in $f_{q_3}g$ are strongly disfavored because if a vector in $f_{q_2}g$ is antiparallel (or close to antiparallel) to one in $f_{q_3}g$, this yields infinite (or merely large) positive contributions to κ_{32} and to κ_{322} and hence to ϵ_c and ϵ_c , meaning that there is an infinite (or large) free energy penalty for $\theta \neq 0$.

Summarizing, we have arrived at two rules for constructing favorable crystal structures for three-flavor crystalline color superconductivity. First, the sets $f_{q_2}g$

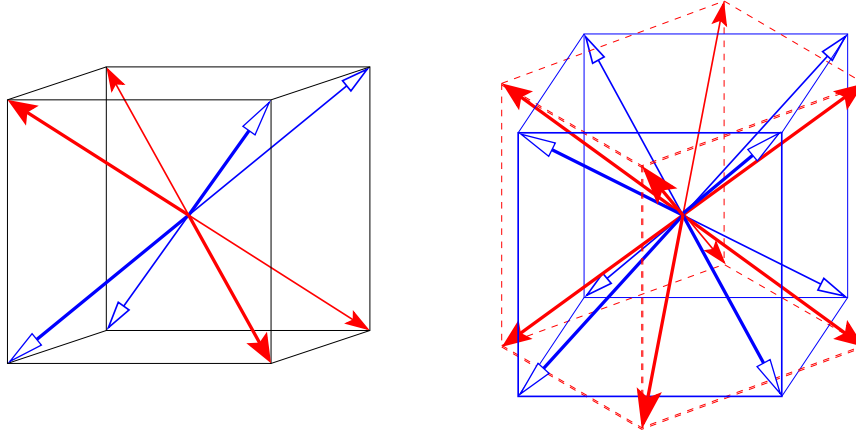


Fig. 5. The momenta that constitute the CubeX (left) and 2Cube45z (right) crystal structures. The set q_3 of hudi pairing momenta is given by the solid-tipped (red online) arrows. The set q_2 of husi pairing momenta is given by the hollow-tipped (blue online) arrows.

and $f_{q_3}g$ should each be chosen to yield crystal structures which, seen as separate two-avor crystalline phases, are as favorable as possible. In Section 3.2.3 we have reviewed how this should be done and the conclusion that the most favored $f_{q_2}g$ or $f_{q_3}g$ in isolation consists of eight vectors pointing at the corners of a cube.⁶⁵ Second, the new addition in the three-avor case is the qualitative principle that $f_{q_2}g$ and $f_{q_3}g$ should be rotated with respect to each other in such a way as to best keep vectors in one set away from the antipodes of vectors in the other set.

3.6. Multiple plane waves

Rajagopalan and Sharma have analyzed 11 different crystal structures,⁵² in each case calculating ϵ_1 and ϵ_2 and ϵ_3 and ϵ_4 , and hence ϵ_1 and ϵ_2 that specify the free energy as in (28). The 11 structures allow one to make many pairwise comparisons that test the two qualitative principles described in Section 3.5. There are some instances of two structures which differ only in the relative orientation of $f_{q_2}g$ and $f_{q_3}g$ and in these cases the structure in which vectors in $f_{q_2}g$ get closer to the antipodes of vectors in $f_{q_3}g$ are always disfavored. And, there are some instances where the smallest angle between a vector in $f_{q_2}g$ and the antipodes of a vector in $f_{q_3}g$ are the same for two different crystal structures, and in these cases the one with them more favorable two-avor structure is more favorable. These considerations, together with explicit calculations, indicate that two structures, which we denote "2Cube45z" and "CubeX", are particularly favorable.

The 2Cube45z crystal momenta are illustrated in Fig. 5, right panel; $f_{q_2}g$ and $f_{q_3}g$ each contain eight vectors pointing at the corners of a cube. If we orient $f_{q_2}g$ so that its vectors point in the $(1; 1; 1)$ directions, then $f_{q_3}g$ is rotated relative to $f_{q_2}g$ by 45° about the z -axis. In this crystal structure, the hudi and husi

condensates are each face-centered cubic, the structure which in isolation is the most favored two-flavor crystal structure.⁶⁵ The relative rotation has been chosen to maximize the separation between any vector in f_{q_2g} and the nearest antipodes of a vector in f_{q_3g} . The color-flavor and position space dependence of the condensate, defined in (17) and (18), is given by

$$\begin{aligned} \chi_{CF}(\mathbf{x})_{ij} = & \frac{1}{2} \left[\cos \frac{2}{a} (\mathbf{x} + \mathbf{y} + \mathbf{z}) + \cos \frac{2}{a} (\mathbf{x} - \mathbf{y} + \mathbf{z}) \right. \\ & + \cos \frac{2}{a} (\mathbf{x} + \mathbf{y} - \mathbf{z}) + \cos \frac{2}{a} (\mathbf{x} - \mathbf{y} - \mathbf{z}) \\ & + \frac{1}{3} \left[\cos \frac{2}{a} \left(\frac{p}{2} \mathbf{x} + \mathbf{z} \right) + \cos \frac{2}{a} \left(\frac{p}{2} \mathbf{y} + \mathbf{z} \right) \right. \\ & \left. \left. + \cos \frac{2}{a} \left(\frac{p}{2} \mathbf{y} + \mathbf{z} \right) + \cos \frac{2}{a} \left(\frac{p}{2} \mathbf{x} + \mathbf{z} \right) \right] \right]; \end{aligned} \quad (31)$$

where i and j are color (flavor) indices and where

$$a = \frac{p}{q} = \frac{4.536}{1.764 M_s^2} \quad (32)$$

is the lattice spacing of the face-centered cubic crystal structure. For example, with $M_s^2 = 100; 150; 200 \text{ MeV}$ the lattice spacing is $a = 72; 48; 36 \text{ fm}$. Eq. (31) can equivalently be written as $\chi_{CF}(\mathbf{x})_{ij} = \frac{1}{2} \chi_{2ij}(\mathbf{r}) + \frac{1}{3} \chi_{3ij}(\mathbf{r})$, with (31) providing the expressions for $\chi_{2ij}(\mathbf{r})$ and $\chi_{3ij}(\mathbf{r})$. A three-dimensional contour plot that can be seen as depicting either $\chi_{2ij}(\mathbf{r})$ or $\chi_{3ij}(\mathbf{r})$ separately can be found in Ref. 65. We have not found an informative way of depicting the entire condensate in a single contour plot. Note also that in (31) and below in our description of the CubeX phase, we make an arbitrary choice for the relative position of $\chi_{3ij}(\mathbf{r})$ and $\chi_{2ij}(\mathbf{r})$. We show in Ref. 52 that one can be translated relative to the other at no cost in free energy. Of course, rotating one relative to the other changes the Ginzburg-Landau coefficients κ_{32} and κ_{322} and hence the free energy.

We now turn to a description of the CubeX crystal structure. We arrive at this structure by reducing the number of vectors in f_{q_2g} and f_{q_3g} . This worsens the two-flavor free energy of each condensate separately, but allows vectors in f_{q_2g} to be kept farther away from the antipodes of vectors in f_{q_3g} . We do not claim to have analyzed all structures obtainable in this way, but we have found one and only one which has a condensation energy comparable in magnitude to the 2Cube45z structure. The CubeX structure is illustrated in Fig. 5, left panel; f_{q_2g} and f_{q_3g} each contain four vectors forming a rectangle. The eight vectors together point toward the corners of a cube. The two rectangles intersect to look like an "X" if viewed end-on. In the CubeX phase, the color-flavor and position space dependence

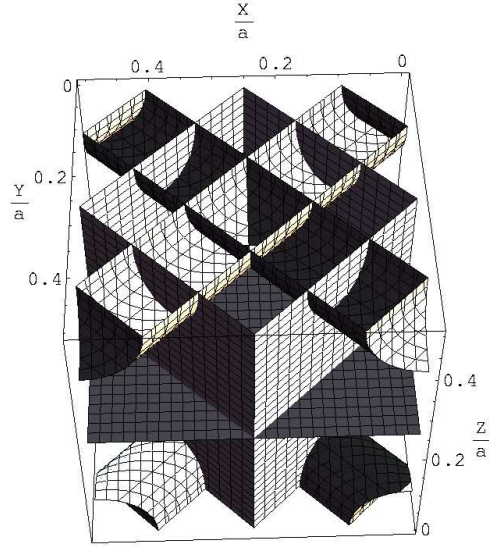


Fig. 6. The CubeX crystal structure of Eq. (33). The figure extends from 0 to $a=2$ in the x , y and z directions. Both $\phi_2(\mathbf{r})$ and $\phi_3(\mathbf{r})$ vanish at the horizontal plane. $\phi_2(\mathbf{r})$ vanishes on the darker vertical planes, and $\phi_3(\mathbf{r})$ vanishes on the lighter vertical planes. On the upper (lower) dark cylinders and the lower (upper) two small corners of dark cylinders, $\phi_2(\mathbf{r}) = +3/3$ ($\phi_2(\mathbf{r}) = -3/3$). On the upper (lower) lighter cylinders and the lower (upper) two small corners of lighter cylinders, $\phi_3(\mathbf{r}) = -3/3$ ($\phi_3(\mathbf{r}) = +3/3$). Note that the largest value of $|\mathbf{j}_1(\mathbf{r})|$ is 4, occurring along lines at the centers of the cylinders. The lattice spacing is a when one takes into account the signs of the condensates; if one looks only at $|\mathbf{j}_1(\mathbf{r})|$, the lattice spacing is $a=2$. a is given in (32). In (33) and hence in this figure, we have made a particular choice for the relative position of $\phi_3(\mathbf{r})$ versus $\phi_2(\mathbf{r})$. In fact, one can be translated relative to the other with no cost in free energy.

of the condensate is given by

$$\begin{aligned} \chi_{ij}(\mathbf{x}) = & \frac{1}{2} \left[\cos \frac{2}{a} (x + y + z) + \cos \frac{2}{a} (x - y + z) \right. \\ & \left. + \cos \frac{2}{a} (x + y - z) + \cos \frac{2}{a} (x - y - z) \right] \end{aligned} \quad (33)$$

We provide a depiction of this condensate in Fig. 6.

We are confident that 2Cube45z is the most favorable structure obtained by rotating one cube relative to another. We are not as confident that CubeX is the best possible structure with fewer than $8+8$ vectors. However, the two most favorable structures that we have found, 2Cube45z and CubeX, are impressively robust and make the case that three-flavor crystalline color superconducting phases are the ground state of cold quark matter over a wide range of densities. If even better crystal structures can be found, this will only further strengthen this case.

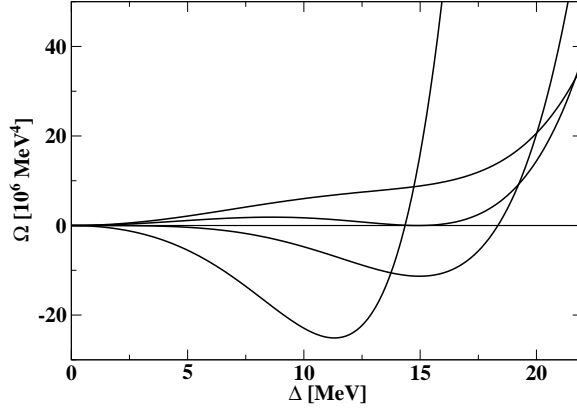


Fig. 7. Free energy vs. Δ for the CubeX crystal structure, described in Section 3.6, at four values of M_s^2 . From top curve to bottom curve, as judged from the left half of the figure, the curves are $M_s^2 = 240, 218.61, 190$, and 120 MeV, corresponding to $\mu = 0.233, 0.140, 0, -0.460$. The first order phase transition occurs at $M_s^2 = 218.61$ MeV. The values of Δ and Ω at the minima of curves like these are what we plot in Figs. 1 and 2.

3.7. Free energy comparisons and conclusions

The gap parameter and free energy (Ω) can be evaluated for all the crystal structures whose Ginzburg-Landau coefficients have been determined.⁵² For a given crystal structure, (Ω) is given by Eq. (27), with μ_e and μ_s taken from Table II of Ref. 52. The quadratic coefficient is related to μ_s by Eq. (25). Recall that we have made the approximation that $\mu_2 = \mu_3 = \mu_s = M_s^2/8$, valid up to corrections of order $M_s^3 = 4$. At any value of M_s^2 , we can evaluate (Ω) and hence (Δ), determine Δ by minimizing Ω , and finally evaluate the free energy at the minimum. In Fig. 7, we give an example of (Ω) for various M_s^2 for one crystal structure with a first order phase transition (CubeX), illustrating how the first order phase transition is found, and how the solving the gap equations | i.e. minimizing Ω | is found. In Figs. 1 and 2, we plot Δ and Ω at the minimum versus M_s^2 for the two most favorable crystal structures that we have found, namely the CubeX and 2Cube45z described in Section 3.6.

In Figs. 1 and 2, we have chosen the interaction strength between quarks such that the CFL gap parameter at $M_s = 0$ is $\mu_0 = 25$ MeV. However, our results for both the gap parameters and the condensation energy for any of the crystalline phases can easily be scaled to any value of μ_0 . Recall that the quartic and sextic coefficients in the Ginzburg-Landau free energy do not depend on μ_0 . And, recall from Eq. (25) that μ_0 enters only through the combination $\mu_{2SC} = \mu_0$, where $\mu_{2SC} = 2^{1/3} \mu_0$ and $\mu_s = M_s^2/8$. This means that if we pick a $\mu_0 \neq 25$ MeV, the curves describing the gap parameters for the crystalline phases in Fig. 1 are precisely unchanged if we rescale both the vertical and horizontal axes proportional to $\mu_0 = 25$ MeV. In the case of Fig. 2, the vertical axis must be rescaled by

($\mu_0 = 25 \text{ MeV}$)². Of course, the weak-coupling approximation $\mu_0 \ll M_s$, which we have used to simplify the calculation of the Ginzburg-Landau coefficients in Ref. 52 will break down if we scale μ_0 to be too large. We cannot evaluate up to what μ_0 we can scale our results reliably without doing a calculation that goes beyond the weak-coupling limit. However, such calculations have been done for the gCFL phase in Ref. 44, where it turns out that the gaps and condensation energies plotted in Figs. 1 and 2 scale with μ_0 and μ_0^2 to good accuracy for $\mu_0 \leq 40 \text{ MeV}$ with $M_s = 500 \text{ MeV}$, but the scaling is significantly less accurate for $\mu_0 = 100 \text{ MeV}$. Of course, for μ_0 as large as 100 MeV , any quark matter in a compact star is likely to be in the CFL phase. Less symmetrically paired quark matter, which our results suggest is in a crystalline color superconducting phase, will occur in compact stars only if μ_0 is smaller, in the range where our results can be expected to scale well.

Fig. 1 can be used to evaluate the validity of the Ginzburg-Landau approximation. The simplest criterion is to compare the μ_0 's for the crystalline phases to the CFL gap parameter μ_0 . This is the correct criterion in the vicinity of the 2nd order phase transition point, where $M_s^2 = (8\pi)^2 \mu_0^2$ as in (29). Well to the left, it is more appropriate to compare the μ_0 's for the crystalline phase to $M_s^2 = (8\pi)^2 \mu_0^2$. By either criterion, the Ginzburg-Landau approximation is at the edge of its domain of validity, a result which we expected based on the general arguments of Section 3.4. Therefore, although we expect that the qualitative lessons that we have learned about the favorability of crystalline phases in three-flavor quark matter are valid, and expect that the relative favorability of the 2Cube45z and CubeX structures and the qualitative size of their gaps and condensation energy are trustworthy, we do not expect quantitative reliability of our results. There is therefore strong motivation to analyze crystalline color superconducting quark matter with these two crystal structures without making a Ginzburg-Landau approximation. It will be very interesting to see whether the Ginzburg-Landau approximation underestimates μ_0 and the condensation energy for the crystalline phases with CubeX and 2Cube45z crystal structures, as it does for the much simpler structure in which $\psi_2(r)$ and $\psi_3(r)$ are each single plane waves.⁷¹

Fig. 2 makes it clear that the three-flavor crystalline color superconducting phases with the two most favored crystal structures that have been found are robust by any measure. Their condensation energies reach about half that of the CFL phase at $M_s = 0$. Correspondingly, these two crystal structures are favored over the wide range of $M_s^2 = \mu_0^2$ seen in Fig. 2 and given in Eq. (4).

Taken literally, Fig. 2 indicates that within the regime (4) of the phase diagram occupied by crystalline color superconducting quark matter, the 2Cube45z phase is favored at lower densities and the CubeX phase is favored at higher densities. Although we do have qualitative arguments why 2Cube45z and CubeX are favored over other phases, we have no qualitative argument why one should be favored over the other. Also, in this context the Ginzburg-Landau approximation is not reliable enough for us to conclude that one phase is favored at higher densities while the

other is favored at lower ones. The proper conclusion from these results is that 2Cube45z and CubeX are the two most favorable phases we have found, that both are robust, that the crystalline color superconducting phase of three-flavor quark matter with one crystal structure or the other occupies a wide swath of the QCD phase diagram, and that their free energies are similar enough to each other that a definitive comparison of their free energies will require a calculation that goes beyond the Ginzburg-Landau approximation that we have used here.

3.8. Implications and Future Work

The purpose of this calculation has been to find candidates for the true ground state of quark matter in the "gCFL window", the range of values of $M_s^2 =$ where calculations that are limited to isotropic phases predict that the gCFL phase is favored. Fig. 2 shows that, according to a Ginzburg-Landau theory keeping terms up to sextic order, in most of this range the gCFL phase can be replaced by a much more favorable three-flavor crystalline color superconducting phase and that these crystalline phases may be favored over a wide range of $M_s^2 =$ above the gCFL window also. Fig. 2 also indicates that at the lower end of the range of $M_s^2 =$, closest to the CFL! gCFL transition, there is a narrow region where it is hard to find a crystalline color superconducting phase with lower free energy than the gCFL phase. This narrow region is thus the most likely place to find a ground state consisting of the gCFL phase augmented by current-carrying meson condensates described in Refs. 14, 18. Except within this window, the crystalline color superconducting phases with either the CubeX or the 2Cube45z crystal structure provide an attractive resolution to the instability of the gCFL phase.

Our Ginzburg-Landau calculation provides reason to speculate that most or possibly all of the quark matter core of a compact star might be in a crystalline color superconducting phase. For example, substituting the quite reasonable values $\mu_0 = 25 \text{ MeV}$ and $M_s = 250 \text{ MeV}$ into Eq. (4) we find that the crystalline phases are favored over the range $240 \text{ MeV} < \mu_0 < 847 \text{ MeV}$. Obviously at the lower density end of this range all quark matter phases are replaced by nuclear matter, and the high end of this range extends far beyond the values $\mu_0 \approx 500 \text{ MeV}$ that are expected in the center of compact stars. We therefore find that with these choices for the parameters the crystalline phase covers the entire range of expected densities of stellar quark matter. Of course, if μ_0 is larger, say $\approx 100 \text{ MeV}$, the entire quark matter core could be in the CFL phase. And, there are reasonable values of μ_0 and M_s for which the outer layer of a possible quark matter core would be in a crystalline phase while the inner core would not. We do not know μ_0 and M_s well enough to predict what phases of quark matter occur in compact stars. However, from our results it is clear that one of the possible configurations of a compact star, ultimately to be confirmed or refuted by astrophysical observations, would involve a quark matter core that is mostly or entirely in a crystalline color superconducting phase.

Now that we have two well-motivated ansätze for the crystal structure of three-flavor crystalline color superconducting quark matter and a good qualitative guide to the scale of λ and μ , we should be able to make progress toward the calculation of astrophysically observable properties of compact stars. For example, we would like to predict the effects of a crystalline color superconducting quark core on the rate at which neutron stars cool by neutrino emission and on the occurrence and phenomenology of pulsar glitches.

For cooling, the relevant microphysical quantities are the specific heat and the neutrino emissivity. The specific heat of the crystalline phases will not be dramatically different from that of unpaired quark matter: it rises linearly with T because of the presence of gapless quark excitations at the boundaries of the regions in momentum space where there are unpaired quarks.⁶⁷ (In contrast, in the gCFL case the heat capacity is parametrically enhanced.⁶) However, the neutrino emissivity should turn out to be significantly suppressed relative to that in unpaired quark matter. The evaluation of the phase space for direct Urca neutrino emission from the CubeX and 2Cube45z phases will be a nontrivial calculation, given that thermally excited gapless quarks occur only on patches of the Fermi surfaces, separated by the (many) pairing rings. (The direct Urca processes $u + e \rightarrow s + \bar{s}$ and $s \rightarrow u + e + \bar{s}$ require s , u and e to all be within T of a place in momentum space where they are gapless and at the same time to have $p_u + p_e = p_s$ to within T . Here, $T \sim 1$ keV is very small compared to all the scales relevant to the description of the crystalline phase itself.)

The idea that a region of a star made of quark matter in a crystalline phase could be the place where (some) glitches originate goes back to Ref. 19, where it was suggested that a crystalline color superconductor condensate could pin rotational vortices. This leads to the possibility that the presence of crystalline quark matter in compact stars could be strongly constrained by comparing their predicted glitch phenomenology with what is actually observed.

There are two key microphysical properties of crystalline quark matter that must be estimated before glitch phenomenology can be addressed: the pinning force on rotational vortices and the shear modulus of the crystal. In order for glitches to occur it is necessary for rotational vortices in some region of the star to be pinned and immobile while the spinning pulsar's angular velocity slows over years. But this can only occur if the pinning force is strong enough to lock the vortices to the crystal structure and if the structure resists deformation, i.e. has a large enough shear modulus. (The glitches themselves are then triggered by the catastrophic unpinning and motion of long-immobile vortices.)

To estimate the pinning force we must analyze how the CubeX and 2Cube45z phases respond when rotated. We expect vortices to form and be pinned at the intersections of the nodal planes at which condensates vanish. This analysis faces two complications. Firstly, baryon number current can be carried by gradients in the phase of either the h_{u} crystalline condensate or the h_{d} condensate or both,

so we must determine which types of vortices are formed. Secondly, the vortex core size, l_v , is only a factor of three to four smaller than the lattice spacing a . This means that the vortices cannot be thought of as pinned by an unchanged crystal; the vortices themselves will qualitatively deform the crystalline condensate in their vicinity.

The second microphysical quantity that is required is the shear modulus of the crystal. This can be related to the coefficients in the low energy effective theory that describes the phonon modes of the crystal.^{62;78;79} This effective theory has been analyzed, and its coefficients calculated, for the two-flavor crystalline color superconductor with face-centered cubic symmetry.⁷⁹ Analyzing the phonons in the three-flavor crystalline color superconducting phases with the 2Cube45z and CubeX crystal structures is thus a priority for future work.

The instability of the gCFL phase was a significant bend in the road to understanding the properties of dense matter, but one that is now receding behind us. With the emergence of two robust crystalline phases, possibly accounting for as much as all of the quark matter that may occur, we can glimpse on the road ahead the microphysical calculations prerequisite to identifying observations that can be used to rule out (or in) the presence of quark matter in a crystalline color superconducting phase within neutron stars.

4. Coda

The project of delineating a plausible phase diagram for high-density quark matter is still not complete. We have discussed some ideas for the "non-CFL" region, but there are others such as a suggested gluon condensation in two-flavor quark matter,¹³ and deformation of the Fermi surfaces (discussed so far only in non-beta-equilibrated nuclear matter⁸⁰). It is very interesting to note that the problem of how a system with pairing responds to a stress that separates the chemical potentials of the pairing species is a very generic one, arising in condensed matter systems and cold atom systems as well as in quark matter. Recent work by Son and Stephanov⁸¹ and Mannarelli, Nardulli and Ruggieri⁸² on a two-species model characterized by a diluteness parameter and a splitting potential shows that between the BCS-paired region and the unpaired region in the phase diagram one should expect a translationally-broken region. In QCD this could correspond to a p-wave meson condensate or a crystalline color superconducting state. What is particularly exciting is that the technology of cold atom traps has advanced to the point where fermion superfluidity can now be seen in conditions where many of the important parameters can be manipulated, and it may soon be possible to investigate the response of the pairing to external stress under controlled experimental conditions. Pairing in a gas of ultracold fermionic atoms can never yield a complete analogue of pairing in dense quark matter, because the atoms are neutral and thus the requirement of neutrality imposes no constraints, whereas we have seen that in the quark matter context imposing both color and electric neutrality is a crucial qualitative

driver for the physics, for example precluding phase separation which can easily happen in the cold atom system. However, even without yielding a complete analogue these experiments could answer qualitative questions of interest. For example, should they discover a translationally broken regime in the absence of rotation, it will be very interesting first to see what crystal structure emerges and second to study the response of such a phase to rotation.

KR acknowledges the hospitality of the Nuclear Theory Group at LBNL. This research was supported in part by the Office of Nuclear Physics of the Office of Science of the U.S. Department of Energy under contracts # DE-AC02-05CH11231, # DE-FG02-91ER50628, # DE-FG01-04ER0225 (OJI) and cooperative research agreement # DF-FC02-94ER40818.

References

1. J. Bardeen, L. Cooper, J. Schrieffer, Phys. Rev. 106, 162 (1957); Phys. Rev. 108, 1175 (1957)
2. M. Alford, K. Rajagopal and F. Wilczek, Nucl. Phys. B 537, 443 (1999) [hep-ph/9804403].
3. For reviews, see K. Rajagopal and F. Wilczek, arXiv:hep-ph/0011333; M. G. Alford, Ann. Rev. Nucl. Part. Sci. 51, 131 (2001) [arXiv:hep-ph/0102047]; D. K. Hong, Acta Phys. Polon. B 32, 1253 (2001) [hep-ph/0101025]. G. Nardulli, Riv. Nuovo Cim. 25N 3, 1 (2002) [arXiv:hep-ph/0202037]; S. Reddy, Acta Phys. Polon. B 33, 4101 (2002) [arXiv:nucl-th/0211045]; T. Schafer, arXiv:hep-ph/0304281; D. H. Rischke, Prog. Part. Nucl. Phys. 52, 197 (2004) [arXiv:nucl-th/0305030]; M. Alford, Prog. Theor. Phys. Suppl. 153, 1 (2004) [arXiv:nucl-th/0312007]; M. Buballa, Phys. Rept. 407, 205 (2005) [arXiv:hep-ph/0402234]; H. c. Ren, arXiv:hep-ph/0404074; I. Shovkovy, arXiv:nucl-th/0410091; T. Schafer, arXiv:hep-ph/0509068; T. Schafer, arXiv:hep-ph/0602067.
4. M. Alford, C. Kouvaris and K. Rajagopal, Phys. Rev. Lett. 92, 222001 (2004) [arXiv:hep-ph/0311286].
5. M. Alford, C. Kouvaris and K. Rajagopal, Phys. Rev. D 71, 054009 (2005) [arXiv:hep-ph/0406137].
6. M. Alford, P. Jotwani, C. Kouvaris, J. Kundu and K. Rajagopal, arXiv:astro-ph/0411560.
7. M. Huang and I. A. Shovkovy, Phys. Rev. D 70, 051501 (2004) [arXiv:hep-ph/0407049]; M. Huang and I. A. Shovkovy, Phys. Rev. D 70, 094030 (2004) [arXiv:hep-ph/0408268].
8. R. Casalbuoni, R. Gatto, M. Mannarelli, G. Nardulli and M. Ruggieri, Phys. Lett. B 605, 362 (2005) [Erratum-ibid. B 615, 297 (2005)] [arXiv:hep-ph/0410401].
9. I. Gannakis and H. C. Ren, Phys. Lett. B 611, 137 (2005) [arXiv:hep-ph/0412015].
10. M. Alford and Q. h. Wang, J. Phys. G 31, 719 (2005) [arXiv:hep-ph/0501078].
11. M. Huang, Phys. Rev. D 73, 045007 (2006) [arXiv:hep-ph/0504235].
12. K. Fukushima, Phys. Rev. D 72, 074002 (2005) [arXiv:hep-ph/0506080].
13. E. V. Gorbar, M. Hashimoto and V. A. Miransky, Phys. Lett. B 632, 305 (2006) [arXiv:hep-ph/0507303].
14. A. Kryjevski, arXiv:hep-ph/0508180; T. Schafer, Phys. Rev. Lett. 96, 012305 (2006) [arXiv:hep-ph/0508190].

15. E. V. Gorbar, M. Hashimoto, V. A. Miransky and I. A. Shovkovy, [arXiv:hep-ph/0602251](#).
16. K. Iida and K. Fukushima, [arXiv:hep-ph/0603179](#).
17. K. Fukushima, *Phys. Rev. D* **73**, 094016 (2006) [[arXiv:hep-ph/0603216](#)].
18. A. Gerhold and T. Schafer, [arXiv:hep-ph/0603257](#).
19. M. G. Alford, J. A. Bowers and K. Rajagopal, *Phys. Rev. D* **63**, 074016 (2001) [[arXiv:hep-ph/0008208](#)].
20. M. G. Alford, J. Berges and K. Rajagopal, *Nucl. Phys. B* **558**, 219 (1999) [[arXiv:hep-ph/9903502](#)]; T. Schafer and F. W. Ilczek, *Phys. Rev. D* **60**, 074014 (1999) [[arXiv:hep-ph/9903503](#)].
21. T. Schafer, *Nucl. Phys. B* **575**, 269 (2000) [[arXiv:hep-ph/9909574](#)].
22. I. A. Shovkovy and L. C. R. Wijewardhana, *Phys. Lett. B* **470**, 189 (1999) [[arXiv:hep-ph/9910225](#)].
23. N. J. Evans, J. Homuzdiar, S. D. H. Hsu and M. Schwetz, *Nucl. Phys. B* **581**, 391 (2000) [[arXiv:hep-ph/9910313](#)].
24. R. D. Pisarski and D. H. Rischke, [nucl-th/9907094](#).
25. M. Iwasaki, T. Iwado, *Phys. Lett. B* **350**, 163 (1995); M. Iwasaki, *Prog. Theor. Phys. Suppl.* **120**, 187 (1995).
26. T. Schafer, *Phys. Rev. D* **62**, 094007 (2000) [[arXiv:hep-ph/0006034](#)].
27. M. Buballa, J. Hosek and M. Oertel, *Phys. Rev. Lett.* **90**, 182002 (2003) [[arXiv:hep-ph/0204275](#)].
28. M. G. Alford, J. A. Bowers, J. M. Cheyne and G. A. Cowan, *Phys. Rev. D* **67**, 054018 (2003) [[arXiv:hep-ph/0210106](#)].
29. A. Schmitt, Q. Wang and D. H. Rischke, *Phys. Rev. D* **66**, 114010 (2002) [[arXiv:nucl-th/0209050](#)].
30. A. Schmitt, *Phys. Rev. D* **71**, 054016 (2005) [[arXiv:nucl-th/0412033](#)];
31. K. Iida and G. Baym, *Phys. Rev. D* **63**, 074018 (2001) [Erratum-*ibid.* **66**, 059903 (2002)] [[arXiv:hep-ph/0011229](#)].
32. P. Amore, M. C. Birse, J. A. McGovern and N. R. Walet, *Phys. Rev. D* **65**, 074005 (2002) [[arXiv:hep-ph/0110267](#)].
33. M. Alford and K. Rajagopal, *JHEP* **0206**, 031 (2002) [[arXiv:hep-ph/0204001](#)].
34. A. W. Steiner, S. Reddy and M. Prakash, *Phys. Rev. D* **66**, 094007 (2002) [[arXiv:hep-ph/0205201](#)].
35. M. Huang, P. f. Zhuang and W. q. Chao, *Phys. Rev. D* **67**, 065015 (2003) [[arXiv:hep-ph/0207008](#)];
36. F. Neumann, M. Buballa and M. Oertel, *Nucl. Phys. A* **714**, 481 (2003) [[arXiv:hep-ph/0210078](#)].
37. P. F. Bedaque and T. Schafer, *Nucl. Phys. A* **697**, 802 (2002) [[arXiv:hep-ph/0105150](#)]; D. B. Kaplan and S. Reddy, *Phys. Rev. D* **65**, 054042 (2002) [[arXiv:hep-ph/0107265](#)]; A. K. Ryževski, D. B. Kaplan and T. Schafer, *Phys. Rev. D* **71**, 034004 (2005) [[arXiv:hep-ph/0404290](#)];
38. A. K. Ryževski and T. Schafer, *Phys. Lett. B* **606**, 52 (2005) [[arXiv:hep-ph/0407329](#)]; A. K. Ryževski and D. Yamada, *Phys. Rev. D* **71**, 014011 (2005) [[arXiv:hep-ph/0407350](#)].
39. T. Schafer, *Phys. Rev. D* **65**, 094033 (2002) [[arXiv:hep-ph/0201189](#)].
40. M. Buballa, *Phys. Lett. B* **609**, 57 (2005) [[arXiv:hep-ph/0410397](#)].
41. M. M. Forbes, *Phys. Rev. D* **72**, 094032 (2005) [[arXiv:hep-ph/0411001](#)].
42. M. Alford, C. Kouvaris and K. Rajagopal, [arXiv:hep-ph/0407257](#).
43. S. B. Ruster, I. A. Shovkovy and D. H. Rischke, *Nucl. Phys. A* **743**, 127 (2004) [[arXiv:hep-ph/0405170](#)].
44. K. Fukushima, C. Kouvaris and K. Rajagopal, *Phys. Rev. D* **71**, 034002 (2005)

- [arXiv:hep-ph/0408322].
45. H. Abuki, M. Kitazawa and T. Kunihito, Phys. Lett. B 615, 102 (2005) [arXiv:hep-ph/0412382].
 46. S.B. Ruster, V.W. erth, M. Buballa, I.A. Shovkovy and D.H. Rischke, Phys. Rev. D 72, 034004 (2005) [arXiv:hep-ph/0503184].
 47. D. Blaschke, S. Fredriksson, H. G. rigorian, A. M. O ztas and F. Sandin, Phys. Rev. D 72, 065020 (2005) [arXiv:hep-ph/0503194].
 48. I. Shovkovy and M. Huang, Phys. Lett. B 564, 205 (2003) [arXiv:hep-ph/0302142];
 49. M. Huang and I. Shovkovy, Nucl. Phys. A 729, 835 (2003) [arXiv:hep-ph/0307273].
 50. E. Gubankova, W. V. Liu and F. Wilczek, Phys. Rev. Lett. 91, 032001 (2003) [arXiv:hep-ph/0304016].
 51. K. Rajagopal and F. Wilczek, Phys. Rev. Lett. 86, 3492 (2001) [arXiv:hep-ph/0012039].
 52. K. Rajagopal and R. Sharma, arXiv:hep-ph/0605316.
 53. P. F. Bedaque, H. Calkas and G. Rupak, Phys. Rev. Lett. 91, 247002 (2003) [arXiv:cond-mat/0306694]; M. M. Forbes, E. Gubankova, W. V. Liu and F. Wilczek, Phys. Rev. Lett. 94, 017001 (2005) [arXiv:hep-ph/0405059]; J. Carlson and S. Reddy, Phys. Rev. Lett. 95, 060401 (2005) [arXiv:cond-mat/0503256].
 54. M. W. Zwierlein, A. Schirotzek, C. H. Schunck, and W. Ketterle, Science 311, 492 (2006) [arXiv:cond-mat/0511197].
 55. G. B. Partridge, W. Li, R. J. Kamar, Y. -a. Liao, and R. G. Hulet, Science 311, 503 (2006) [arXiv:cond-mat/0511752].
 56. S. Reddy and G. Rupak, Phys. Rev. C 71, 025201 (2005) [arXiv:nucl-th/0405054].
 57. D. Bailin and A. Love, Phys. Rept. 107, 325 (1984).
 58. M. G. Alford, K. Rajagopal and F. Wilczek, Phys. Lett. B 422, 247 (1998) [arXiv:hep-ph/9711395].
 59. R. Rapp, T. Schafer, E. V. Shuryak and M. Velkovsky, Phys. Rev. Lett. 81, 53 (1998) [arXiv:hep-ph/9711396].
 60. K. Rajagopal and A. Schmitt, Phys. Rev. D 73, 045003 (2006) [arXiv:hep-ph/0512043].
 61. J. A. Bowers, J. Kundu, K. Rajagopal and E. Shuster, Phys. Rev. D 64, 014024 (2001) [arXiv:hep-ph/0101067].
 62. R. Casalbuoni, R. Gatto, M. Mannarelli and G. Nardulli, Phys. Lett. B 511, 218 (2001) [arXiv:hep-ph/0101326].
 63. A. K. Leibovich, K. Rajagopal and E. Shuster, Phys. Rev. D 64, 094005 (2001) [arXiv:hep-ph/0104073].
 64. J. Kundu and K. Rajagopal, Phys. Rev. D 65, 094022 (2002) [arXiv:hep-ph/0112206].
 65. J. A. Bowers and K. Rajagopal, Phys. Rev. D 66, 065002 (2002) [arXiv:hep-ph/0204079].
 66. R. Casalbuoni and G. Nardulli, Rev. Mod. Phys. 263, 320 (2004) [arXiv:hep-ph/0305069].
 67. R. Casalbuoni, R. Gatto, M. Mannarelli, G. Nardulli, M. Ruggieri and S. Stramaglia, Phys. Lett. B 575, 181 (2003) [Erratum -ibid. B 582, 279 (2004)] [arXiv:hep-ph/0307335].
 68. R. Casalbuoni, M. Cinale, M. Mannarelli, G. Nardulli, M. Ruggieri and R. Gatto, Phys. Rev. D 70, 054004 (2004) [arXiv:hep-ph/0404090].
 69. R. Casalbuoni, R. Gatto, N. Ippolito, G. Nardulli and M. Ruggieri, Phys. Lett. B 627, 89 (2005) [arXiv:hep-ph/0507247].
 70. M. Cinale, G. Nardulli, M. Ruggieri and R. Gatto, Phys. Lett. B 636, 317 (2006) [arXiv:hep-ph/0602180].

71. M. Mannarelli, K. Rajagopal and R. Sharma, *arXiv hep-ph/0603076*.
72. A. I. Larkin and Yu. N. Ovchinnikov, *Zh. Eksp. Teor. Fiz.* 47, 1136 (1964) [*Sov. Phys. JETP* 20, 762 (1965)]; P. Fulde and R. A. Ferrell, *Phys. Rev.* 135, A550 (1964); S. Takada and T. Izuyama, *Prog. Theor. Phys.* 41, 635 (1969).
73. D. K. Hong, *arXiv hep-ph/0506097*.
74. M. Alford and Q. H. Wang, *J. Phys. G* 32, 63 (2006) [*arXiv hep-ph/0507269*].
75. M. G. Alford and G. A. Cowan, *J. Phys. G* 32, 511 (2006) [*arXiv hep-ph/0512104*].
76. M. G. Alford, K. Rajagopal, S. Reddy and F. Wilczek, *Phys. Rev. D* 64, 074017 (2001) [*arXiv hep-ph/0105009*].
77. A. Gerhold and A. Rebhan, *Phys. Rev. D* 68, 011502 (2003) [*arXiv hep-ph/0305108*]; A. Krywinski, *Phys. Rev. D* 68, 074008 (2003) [*arXiv hep-ph/0305173*]; A. Gerhold, *Phys. Rev. D* 71, 014039 (2005) [*arXiv hep-ph/0411086*]; D. D. Dietrich and D. H. Rischke, *Prog. Part. Nucl. Phys.* 53, 305 (2004) [*arXiv nucl-th/0312044*];
78. R. Casalbuoni, R. Gatto, M. Mannarelli and G. Nardulli, *Phys. Rev. D* 66, 014006 (2002) [*arXiv hep-ph/0201059*].
79. R. Casalbuoni, E. Fabiano, R. Gatto, M. Mannarelli and G. Nardulli, *Phys. Rev. D* 66, 094006 (2002) [*arXiv hep-ph/0208121*].
80. A. Sedrakian, *arXiv nucl-th/0312053*.
81. D. T. Son and M. A. Stephanov, *arXiv cond-mat/0507586*.
82. M. Mannarelli, G. Nardulli and M. Ruggieri, *arXiv cond-mat/0604579*.